EVs@Scale
U.S. Department of Energy

High-Power Electric Vehicle Charging Hub Integration Platform (eCHIP)

Design Guidelines and Specifications for DC Distribution-Based Charging Hub

Mithat John Kisacikoglu[1], Jason D. Harper[2], Rajendra Prasad Kandula[3], Alastair P. Thurlbeck[1], Akram Syed Ali[2], Emin Ucer[1], Edward Watt[1], Md Shafquat Ullah Khan[1], and Rasel Mahmud[1]

[1]National Renewable Energy Laboratory
[2]Argonne National Laboratory
[3]Oak Ridge National Laboratory

April 2024

U.S. DEPARTMENT OF ENERGY | Office of ENERGY EFFICIENCY & RENEWABLE ENERGY

Disclaimer

List of Acronyms

AC	alternating current
ADMS	advanced distribution management system
Argonne	Argonne National Laboratory
BMS	battery management system
BOM	bill of materials
BPT	bidirectional power transfer
CAN	controller area network
CHB	cascaded H-bridge
COTS	commercial off-the-shelf
CSMS	charge station management system
DAB	dual-active bridge
DBC	database CAN
DC	direct current
DC LC	DC load center
DC-REDB	DC Research Electrical Distribution Bus
DERMS	distributed energy resource management systems
DOE	U.S. Department of Energy
DR	demand response
eCHIP	High-Power Electric Vehicle Charging Hub Integration Platform
EMC	electromagnetic compatibility
EMI	electromagnetic interference
ESIF	Energy Systems Integration Facility
ESS	energy storage system
EV	electric vehicle
EVSE	electric vehicle supply equipment
GaN	gallium nitride
HD	heavy-duty
HPC	high-power charging
IEC	International Electrotechnical Commission
IEEE	Institute of Electrical and Electronics Engineers

IoT	internet of things
ISO	International Organization for Standardization
JSON	JavaScript Object Notation
LD	light-duty
LV	low-voltage
LVDC	low-voltage direct current
MD	medium-duty
MPPT	maximum power point tracking
MRCD	mobile RCD
MV	medium-voltage
MVDC	medium voltage direct current
NAVSEA	Naval Sea Systems Command
NPC	neutral-point clamped
NREL	National Renewable Energy Laboratory
OCPP	Open Charge Point Protocol
OpenADR	Open Automated Demand Response
OpenFMB	Open Field Message Bus
ORNL	Oak Ridge National Laboratory
PLC	power line communication
PV	photovoltaic
RCD	REDB connection device
SECC	supply equipment communications controller
SEMS	site energy management system
SiC	silicon carbide
SOAP	Simple Object Access Protocol
SpEC	Smartgrid EV Communication
SPM	single phase modulation
SSCB	solid-state circuit breaker
SST	solid-state transformer
UPER	Universal Power Electronics Regulator
V2G	vehicle-to-grid

V2X	vehicle-to-everything
ZSM	zero state modulation
ZVS	zero voltage switching

Executive Summary

Managed under the U.S. Department of Energy (DOE)-funded EVs@Scale Consortium, the High-Power Electric Vehicle Charging Hub Integration Platform (eCHIP) project aims to create an experimental platform for integration and control approaches in a direct current (DC), distribution-based high-power charging (HPC) system. The eCHIP project addresses the crucial need to design and validate efficient, low-cost, reliable, and interoperable solutions for a DC-coupled charging hub ("DC hub" for short).

This report explains the design, development, and implementation process of an experimental platform for the DC hub. DC distribution holds significant potential for enhancing the operation of an HPC station architecture. However, there are challenges in establishing a DC hub, including interoperability, commoditization, distributed energy resource integration, stability, DC protection, and a lack of common system-level controllers. To address these challenges, a testing setup is required that accommodates commercial off-the-shelf (COTS) products, as well as novel, in-house designed solutions, to evaluate different use cases at rated power and voltage levels.

The developed setup features a dedicated DC distribution system, DC-DC chargers, electric vehicles, DC loads/sources, protection, and an open-source site energy management system (SEMS). The integrated platform provides a versatile testing environment to address technology and interoperability gaps, and it implements an SEMS. This platform enables comprehensive and robust testing of COTS devices, charger prototypes, SEMS controllers, and protection schemes, which together will accelerate the transition to electric vehicles (EVs) at scale. This report does not claim to be comprehensive in covering all possible aspects of designing a DC hub. Rather, the document aims to provide a guideline on important metrics and considerations when designing such a system, and it provides insights on the first experimental results attained in the eCHIP project.

The eCHIP DC hub is tested for various use cases. The important hardware ratings used within the scope of this report include 950-V DC bus voltage, a 660-kW grid-tied inverter, a 150-kW COTS charger, a 175-kW in-house developed DC-DC charger, an emulated 100-kW battery energy storage system (ESS), an emulated 250-kW photovoltaic (PV) system, and a 500-kW building load emulation.

The highlights of the report can be summarized as follows:

- An in-depth review of available power architecture, control, and communication methods for a DC hub is conducted.
- EV charging connected with battery ESS, a PV system, and building loads demonstrates the functionality of the combined DC hub platform at the National Renewable Energy Laboratory's Energy Systems Integration Facility.
- A 175-kW, 1000-V class DC-DC Universal Power Electronics Regulator (UPER) is developed by Oak Ridge National Laboratory.
- The custom Smartgrid EV Communication, or "SpEC," controller module developed by Argonne National Laboratory shows enhanced integration with DC-DC chargers including the UPER DC-DC converter.
- Bidirectional power transfer with the International Organization for Standardization's ISO 15118-2 is implemented on an electric bus by Argonne and supports further use cases for a DC hub.

The developed proof-of-concept charging platform and open-source SEMS allow the development and testing of various controllers and chargers from different vendors. The DC hub platform integrated EVs, an ESS, a PV system, and building load to demonstrate the flexibility of the platform. The open-source SEMS controlled the devices within the hub using a rule-based implementation, realizing available standards.

Table of Contents

List of Figures

List of Tables

1 Introduction

Increasing electric vehicle (EV) adoption will change the composition of EV charging load toward high-power charging (HPC). This trend will continue as more medium-duty (MD) and heavy-duty (HD) vehicle applications are electrified, and as all EV categories, including light-duty (LD) vehicles, become capable of faster charging. These shifts provide an opportunity for HPC and facility equipment to evolve and improve in efficiency, cost, and size.

HPC stations require a common approach to a scalable and cost-efficient charging hub (Figure 1). The hub should accommodate long- and short-dwell charging of LD, MD, and HD vehicles across many vocations and site configurations (loads and resources). The U.S. Department of Energy (DOE) established the EVs@Scale Consortium, [1] which brings together national laboratories and key stakeholders, to conduct infrastructure research and development to address challenges and barriers for high-power EV charging infrastructure. The goal is to enable greater safety, grid operation reliability, and consumer confidence.

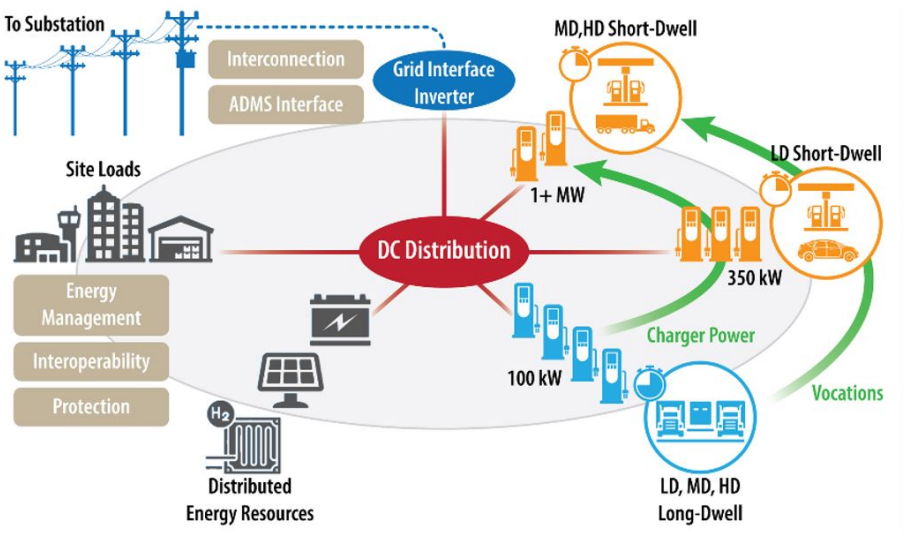

Figure 1. High-power electric vehicle charging hub integration platform

This report details the design and development of a high-power, interoperable charging experimental testbed under the High-Power Electric Vehicle Charging Hub Integration Platform (eCHIP) project within the EVs@Scale Consortium. The eCHIP project is a multiyear effort conducted by Argonne National Laboratory (Argonne), National Renewable Energy Laboratory (NREL), and Oak Ridge National Laboratory (ORNL) [2]. The report summarizes the integration approaches and technology solutions under the concept of a direct current (DC) charging hub (a terminology denoting DC-coupled HPC stations), available in the industry and found in the literature, from field practicality and implementation points of view. The report also explains the eCHIP project team's approach to developing a DC charging hub experimental platform. This report does not claim to be comprehensive in covering all possible aspects of designing a DC charging hub. Rather, the document aims to provide a guideline on important metrics and considerations when designing such a system.

This report describes (1) an overview, background, and various relative standards on DC charging hub approaches; (2) the development of DC charging hub power, control, and communcation components; (3) the development and implementation of a site energy management system (SEMS); and (4) hub component functionality testing results. Figure 2 shows the structure of the report. Chapter 2 addresses the background review on the technology. Chapter 3 discusses the development approach taken by the three national laboratories in the eCHIP project. Chapter 4 provides information about the SEMS; Chapter 5 provides insights on the preliminary hardware implementation results; and Chapter 6 concludes the report and explains the future work.

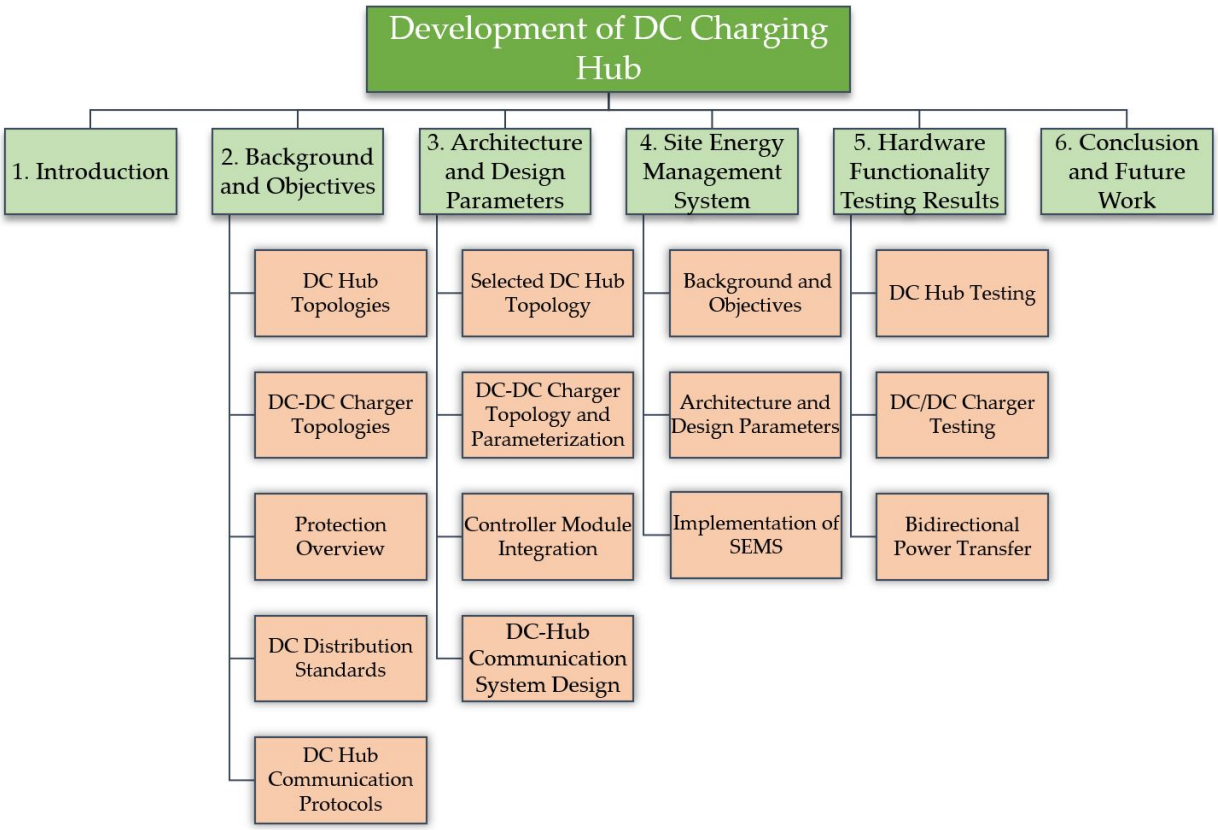

Figure 2. Project report structure

2 Background and Objectives

2.1 Overview of DC Charging Hub Technologies

2.1.1 DC Hub vs. AC Hub – A Comparative Outlook

Most commercially available HPCs are designed to be supplied from a three-phase alternating current (AC) connection. These chargers must incorporate galvanic isolation, achieve high-efficiency AC-DC power conversion, and facilitate a broad spectrum of vehicle battery voltages at their output. While early EVs had generally low battery pack voltage ranging from 300 V to 400 V, some recent EVs have nominal battery pack voltage as high as 800 V. With these challenges taken together, chargers must incorporate multiple conversion stages, filtering, and isolation via low or high-frequency transformers [3]. When multiple HPC stations are co-located to form a charging site, the individual chargers share an AC interconnection. Often this lower-voltage AC (e.g., 480 V) is interfaced with the medium-voltage (MV) utility grid via a distribution transformer. Considering the high stress that an HPC station places on the local utility grid, on-site energy storage and even distributed generation can be incorporated into the charging site design [4]. Connecting all the different assets on the common AC bus can be referred as an "AC hub." However, like the EV battery, energy storage system (ESS) and photovoltaic (PV) generation are inherently DC systems. Therefore, interfacing these systems with the charging station's AC-coupled bus typically requires multiple conversion stages [5].

The DC nature of the HPC station loads, storage, and generation have popularized the concept of an HPC station with a DC-coupled bus, which we refer to as a "DC hub." Figure 3 shows the difference in charging station architecture between the AC and DC hubs. The DC hub architecture is like that of a DC microgrid, though it does not necessarily include generation or storage. Indeed, DC microgrids (as they are well studied for other applications) have widely recognized advantages over the comparable AC solution—namely, reduced costs, increased efficiency, and simplified control [5]. Additionally, the recent rise of wide-bandgap semiconductor technologies such as silicon carbide (SiC) or gallium nitride (GaN) devices has enabled the efficient integration of high-frequency isolation transformers in high-frequency switching converters such as the dual-active bridge (DAB) DC-DC converter. Such topologies strengthen the case for a DC-coupled HPC station, since the EV chargers, energy storage, and PV systems can all connect to the bus with a single, isolated DC-DC conversion stage. That said, the DC hub approach also brings some implementation challenges, such as DC protection, commercial product availability, and standardization.

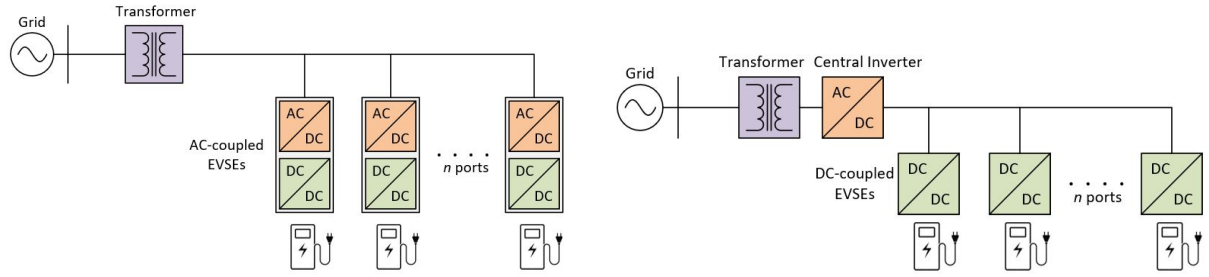

(a) AC hub charging station **(b) DC hub charging station**

Figure 3. AC- and DC-coupled HPC station architectures

The advantages of the DC hub approach can be listed as follows:

- The central inverter and grid-connection transformer can be sized to meet the average charging demand, rather than the peak [6, 7][1].
- DC hubs have fewer power-electronic conversion stages than an AC hub when energy storage or renewable generation are incorporated. Therefore, they provide reduced size and cost, and increased efficiency [5, 8, 9, 10, 11].

[1]Note that a similar advantage also applies to an AC hub with storage when compared to an AC charging station with no storage. However, when the ESS is ignored, due to the stochasticity of charging events and nonlinear nature of charging profiles, the central inverter can be sized for average charging demand, while an AC hub needs to meet maximum demand per port for large charging facilities for the same charging service quality (i.e. charging speed).

- DC hubs have one (or multiple parallel) central inverter(s) with grid-side filters compared to the AC hub, which has a decentralized inverter and an associated grid-side filter at each charger. Therefore, the size and cost of passive components in a DC hub is reduced compared to an AC hub (for the same total power rating) [12].
- DC hubs have simplified controls, since the chargers are coupled via a DC bus [10, 12]. The more complex controls, such as grid synchronization, reactive power control/power factor correction, and required grid support functions, are centralized. There is improved scalability in a DC hub, since individual hub components have a straightforward interface with stable DC voltage. The DC bus voltage can also be used for DC power signaling/communication with distributed controllers.
- There is no reactive power flow in the DC hub, which may lead to more efficient power transmission within the hub's distribution bus [10].
- The central inverter can offer grid support functions such as reactive power compensation at the grid connection [13].
- DC hubs offer a simpler platform for islanded operation during grid faults when energy storage and renewables are integrated [14]. While in grid-connected mode or transitioning between islanded and grid-connected mode, grid voltage and frequency synchronization is isolated to the centralized inverter, which has less impact on the hub distribution bus stability and does not require coordination with generation and storage converters [15].
- DC hub chargers use high-frequency transformers for galvanic isolation, which reduces cost and size for magnetics compared to AC chargers, which may use low-frequency isolation transformers[2].
- DC hubs can use an MV AC solid-state transformer (SST) design to eliminate the low-frequency distribution transformer. The SST is often realized as a cascaded H-bridge (CHB) multilevel converter cascaded with paralleled DAB stages incorporating high-frequency transformers [16, 17, 18]. While AC hubs can also implement an SST in place of the low-frequency distribution transformer, AC-AC SSTs typically use an additional conversion stage compared to AC-DC SSTs [19].
- DC hubs offer advantages to the grid with peak-shaving or load-shifting, made possible when energy storage is integrated into the hub [10][3].

On the other hand, some disadvantages of the DC hub approach can be listed as follows:

- It is more challenging to safely interrupt DC current than AC, since DC current has no zero-crossings. However, DC circuit breakers are uniquely designed to extinguish DC current arcs, and solid-state circuit breakers (SSCBs) are an emerging solution that use small power-electronic devices and commutation circuitry to interrupt the current.
- DC hubs must use a central inverter at the point of grid connection in addition to any grid-connection transformer. The power electronics introduce a significant reliability concern, since they are a single point of failure for the hub [20], and the reliability of a power-electronic converter is typically worse than that of a transformer due to the complexity of the controls and high-frequency switching. That said, the DC hub can implement the central inverter as paralleled converter stages or multiple inverters to improve system redundancy.
- There is a lack of commercially available products designed for DC charging hubs, such as DC-coupled electric vehicle supply equipment (EVSE) and DC-coupled PV converters that integrate maximum power point tracking (MPPT). However, as the technology becomes more mature, more products that are compatible with a DC charging hub approach are expected.
- There are a lack of standards for DC hub product development, which negatively affects the interoperability of the various DC hub components. In Section 2.4, we will summarize the available standards in other industries that a DC charging hub approach could benefit from.

[2] However, some AC hub charger topologies also use a high-frequency transformer approach, with the method used being topology-specific [3].

[3] Note that the same advantage also applies to an AC hub with storage when compared to an AC charging station with no storage.

2.1.2 Different Types of DC Hub Topologies

As shown in Figure 4, a DC hub can have a unipolar or bipolar DC bus. While unipolar remains the most common DC hub architecture, researchers have proposed alternative converter topologies and balancing schemes to realize bipolar DC-coupled charging stations. The bipolar DC bus offers the following advantages over unipolar systems:

- **Increased voltage flexibility:** Chargers and other DC hub components can be connected across either half of the bipolar bus (between positive and neutral or negative and neutral), or across the entire bus (between the positive and negative poles). In other words, full or half voltage can be used [21, 22, 23]. This option provides increased flexibility to supply lower DC-bus voltage to lower-power and longer dwell-time charging demands.
- **Improved fault characteristics:** The availability of the neutral wire enables the use of a TN-S grounding system that allows pole-ground faults to be easily detected and cleared [24].
- **Improved redundant operation:** If one pole is faulted, the other pole can remain operational. However, this redundancy also depends on the nature of the fault. If the bipolar bus is implemented using two independent 2-level inverters connected in cascade, as shown in Figure 4c, then this half-power system redundancy also includes the central inverter.
- **Increased power handling ability:** Chargers that are rated for half of the DC bus voltage can also be used.

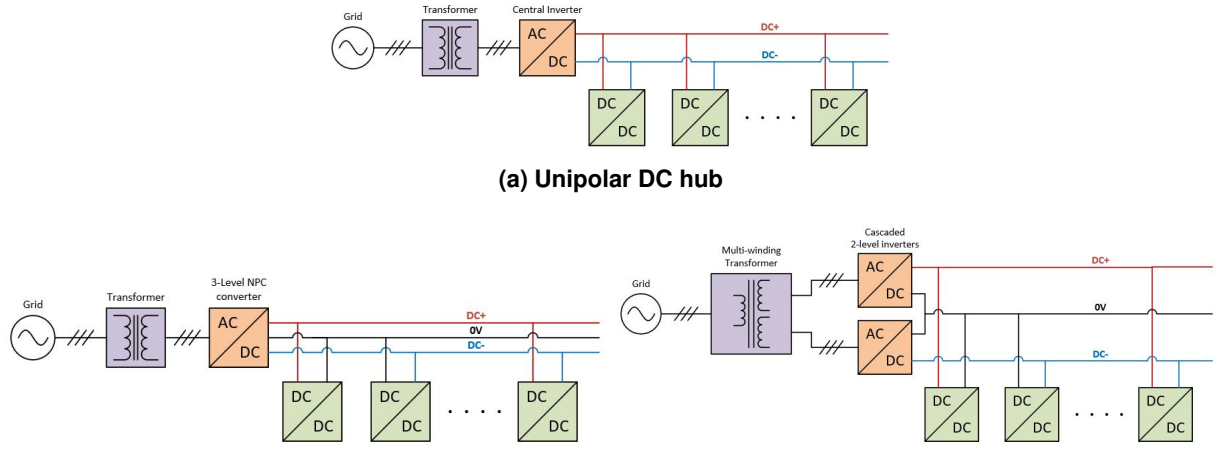

(a) Unipolar DC hub

(b) Bipolar DC hub with 3-level NPC converter (additional balancing circuitry required)

(c) Bipolar DC hub with cascaded 2-level inverters

Figure 4. Unipolar and bipolar DC hub architectures

On the other hand, bipolar charging station design suffers from a voltage imbalance issue, which occurs when an unequal load on each pole of the bus disrupts the bus voltage balance. Most researchers propose voltage balancing control, such as additional balancing circuitry used in conjunction with a three-level neutral-point clamped (NPC) central converter in the bipolar charging station design of [21]. While a multitude of bipolar bus converter topologies and associated balancing schemes can be used, a simpler solution is to use two separately controlled two-level inverters connected in cascade to form the bipolar bus, as shown in Figure 4c. This removes the balancing issue entirely, forming the central inverter out of two discrete inverters that require their own transformers to the utility connection (or use of a multiple-winding transformer, as indicated in Figure 4c) [23].

Considering the high-power level of the DC hub charging station—1 MW or more—researchers have considered alternative strategies for its direct connection to the MV utility grid. Conventionally, the DC hub's central inverter would connect to low-voltage (LV) AC (e.g., 480 V). Then, a distribution transformer connects the hub to the MV distribution system (e.g., 13.8 kV). However, to eliminate the bulky low-frequency distribution transformer, researchers have proposed an SST approach, where a CHB multilevel converter directly connects to the MV distribution system [16, 17, 18]. Then, each module of the CHB is connected to a DAB converter that includes a high-frequency transformer. Since the DAB converters are isolated, their outputs for each phase are combined in parallel. Therefore, the high step-down ratio is achieved by a series-input parallel-output converter configuration, in addition

to the step-down ratio implemented within each DAB converter. By moving from low- to high-frequency isolation, the size and cost of the transformer magnetics may be reduced in this approach. This study does not aim to uncover the advantages/disadvantages between LV or direct MV interconnection to the utility grid. Rather, we focus on how the combined inverter, DC hub, and DC-DC chargers operate, and we summarize possible methods to control the system operation with charging requirements in mind.

2.2 Overview of DC-DC Charger Topologies Available for DC Charging Hub

This section lists some of the well-known DC-DC converter topologies available for the DC charging hub. The major requirements for DC chargers are stable primary voltage/current control algorithms, isolation from the DC charging hub, improved power density to reduce footprint, and scalability in a modular way. Furthermore, bidirectional operation is required to improve vehicle-to-everything (V2X) functionality. Charger weight is also an important consideration for improving ease of maintenance. One method to reduce charger weight or to improve power density is to implement the isolation at high frequency instead of using typical 60-Hz low frequency. However, designing such high-frequency isolation transformers at high currents—up to 500 A for 175-kW or 350-kW modules—while considering the thermal effects (e.g., cooling) is a major challenge.

Regarding scalability, charger modules are typically operated in parallel to achieve higher power. However, there are practical limits to how many modules can be operated in parallel in a single DC charger. One example of the practical limits is the limitation on the communication bandwidth between a central controller and multiple parallel connected modules. The central controller here transfers the start/stop and reference set-point commands and receives the status from each charger module.

At the consumer level, the charger should be compatible with both 400-V class and 800-V class vehicles, i.e., the charger module should be capable of operating at a voltage range of 200 V to 900 V. For HD EVs, the voltage is expected to reach 1,500 V. Inverter technology at 1,500 V is well established and is driving the PV industry. However, high-power isolated converters at 1,500 V are still a nascent technology.

There are predominantly three types of topologies to implement isolated DC-DC chargers, as shown in Figure 5. All the configurations consist of two active bridges interconnected through a medium-frequency transformer. The LLC (Inductor-Inductor-Capacitor) converter is a type of series-resonant converter and is commonly employed. In this configuration, the secondary bridge is shown as a diode bridge to save costs. Alternatively, the diode bridge may be replaced with active semiconductor switches to achieve synchronous rectification, and thereby improved efficiency. The DAB converter relies on the series inductance and phase shift between the two bridges for power transfer. The CLLC (Capacitor-Inductor-Inductor-Capacitor) converter builds on LLC converter to add bidirectional functionality.

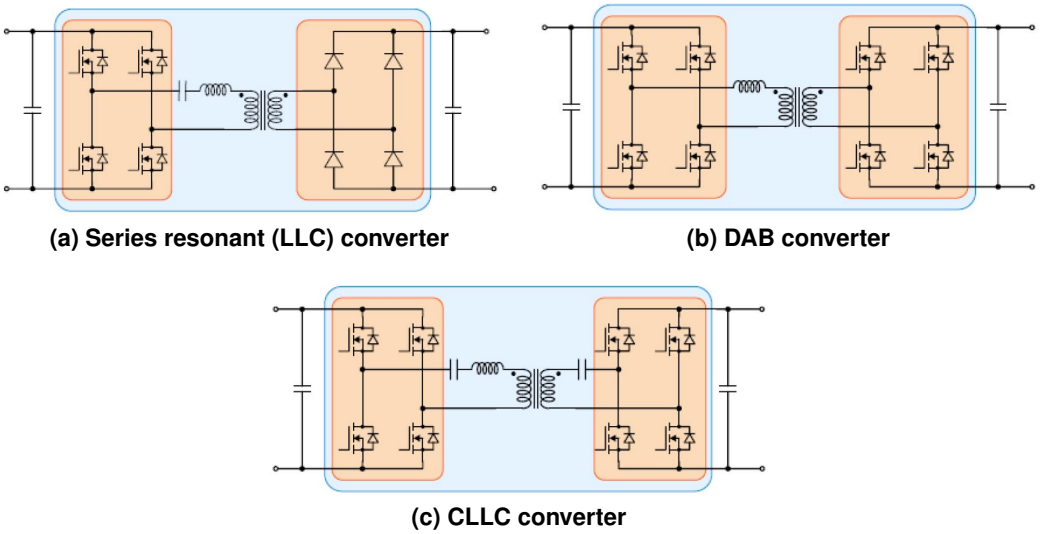

(a) Series resonant (LLC) converter

(b) DAB converter

(c) CLLC converter

Figure 5. Possible isolated DC-DC converters for charging application

A comparison of all the topologies described above is provided in Table 1 below. The LLC converter has the advantage of achieving zero voltage switching (ZVS), which results in lower loss and inherently blocks DC offsets that could be damaging for the transformer. However, it is not ideally suited for bidirectional operation and needs a larger output capacitor compared to a DAB converter. The CLLC converter adds bidirectional functionality to the LLC converter through symmetricity, but it is relatively complex to achieve wide voltage control capability. The DAB converter has solid control capability, smaller filter capacitors, and is inherently bidirectional. However, managing, sensing, and controlling the DC bias currents in the high-frequency isolation transformer—which can otherwise lead to transformer saturation and loss of controllability—are major challenges. Each converter has merits and demerits. However, the concerns with the DAB converter can be addressed through controls, so it was chosen for the charger.

Table 1. Comparison of Different DC-DC Charger Topologies

Parameter	Converter Type		
	LLC	**DAB**	**CLLC**
Efficiency: ZVS range	Not good for wide voltage range	Not good for wide voltage range	Not good for wide voltage range
Controllability: Light load power regulation	Medium	High	Medium
DC bias currents– transformer saturation	Caps block DC	Control-based	Caps block DC
Voltage/current stress	Resonant cap has high voltage stress	Low	Resonant cap has high voltage stress
Bidirectionality	Not well suited	Suitable	Suitable
Output current ripple	Large filter cap required	Low	Large filter cap required
Leakage inductor	Small	Relatively larger: high circulating reactive power	Small
Medium frequency transformer stress	Sinusoidal voltages	Square voltages	Sinusoidal voltages

*Green: Advantageous; Yellow: Manageable; Red: Major constraint

2.3 DC Hub Protection Overview

This section presents a brief overview of the system-level protection challenges in DC charging hubs. Some of the major challenges that DC charging hubs will face in terms of protection include the following:

- **Detection of faults.** When the power electronics systems cannot source large fault current, i.e., the typical fault currents are less than 2.0 per unit, the detection of faults becomes more challenging. In addition, the absence of frequency and phasor information in DC systems makes it difficult for fault detection and localization.
- **Fault interruption.** This is especially challenging in DC systems due to the following:
  1. The absence of natural zero crossing is a challenge to extinguish the arc during breaker opening.
  2. Capacitors discharge rapidly when a fault occurs. As a result of the fast fault current, the DC bus voltage drops quickly if the fault is not cleared. Therefore, fault interruption must be fast enough to handle a very fast fault current rise.
- **Identification of possible fault mechanisms.** The type and diversity of the components in DC hubs, such as grounding type, AC-DC converter topologies, DC-DC converter types, and DC distribution system configuration (i.e., radial, ring, unipolar, bipolar, etc.) will cause the fault mechanisms to differ.
- **Analyzing the impact of faults on the system.** This requires a study to identify where the fault currents are catastrophic without additional protection elements such as circuit breakers, fuses, etc.
- **Categorization of faults.** Some faults, such as line-to-ground in a floating DC system, are benign and do not need fast detection and large fault current interruption capability. On the other hand, a short circuit between the DC pole terminals may need fast detection and large fault current interruption capability. Categorization will

help identify where fast circuit breakers are required and where nominal current disconnectors/contactors are sufficient.

- **Lack of mature standards**. The immaturity of standardization for DC charging hub protection is another challenge.

To ensure safe and reliable operation of a DC charging hub, the protection system needs to perform three functions: i) fault detection, ii) fault isolation, and iii) fault reconfiguration [25]. Figure 6 shows the overall framework for the DC hub fault management approach that will be followed in this project.

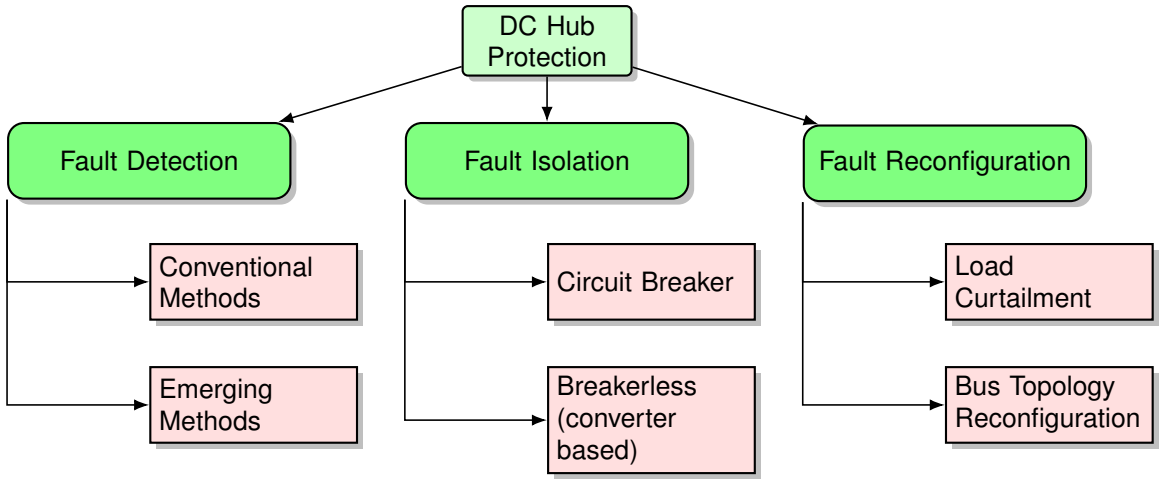

Figure 6. Overview of DC hub fault management

2.3.1 Fault Types in a DC Charging Hub

The major system-level possible fault types in a DC charging hub (based on unipolar configuration) are pole-pole, pole-ground, and AC grid faults. Within those faults, the most common type of fault observed in such systems is the pole-ground fault [25]. The impedance of a pole-pole fault is usually low, whereas the pole-ground fault impedance can be either low or high [26]. The fault impedance has a significant impact on the severity of the fault current and fault detection.

Pole-pole faults can be considered a low impedance load for the DC hub. These types of faults are the most severe faults for a DC hub, as the fault current is very high due to low impedance. The fault current of the pole-pole fault in the DC hub has two components: transient and steady-state. The capacitors in the DC hub and the converters contribute to the high amplitude transient fault current. The transient fault current causes the DC hub voltage to drop, and a fault current conduction path through the forward-biased diodes can contribute to the steady-state fault current [25, 26].

Depending on the grounding configuration, the pole-ground fault characteristics can vary widely. For a low impedance fault, the pole-ground fault current characteristics could be very similar to pole-pole fault current. However, for a high impedance fault, a fault current path though the forward biased diodes,might be absent. It is worth pointing out that the actual fault current for both pole-pole and pole-ground faults will also be heavily dependent on the converter topology and network impedance.

2.3.2 Impact of Converter Design on DC Fault Current

All the converters used in the DC hub contribute to the fault current if there is any fault in the DC hub. Depending on the converter topology and protection features, the fault current contributions from the converters will vary by a significant margin. Additionally, it is important to consider the current limit of the primary energy source, (i.e., grid, ESS, etc.) connected by the converters to the DC hub while estimating the fault current contribution by each converter.

2.3.3 Grounding Requirements

There are many factors that determine the grounding in a DC hub, including design strategy, leakage current, ground fault identification, and equipment safety under fault conditions [27, 28]. The grounding arrangement can help

minimize stray currents and avoid unsafe transient overvoltage conditions [29]. Aside from the grounding configuration, the ground impedance's impact on the converter fault ride-through capabilities needs to be considered. High impedance grounding or ungrounded systems offer greater flexibility to the converters to ride through faults [30]. Aggregated pole-ground capacitance and network impedance during a fault transient can cause undamped oscillatory overvoltage response that leads to instability.

2.4 DC Power Distribution Standards in Other Industries

The need for standardization in high-power charging is driven by rated product availability, safety requirements, interoperability, and efficiency. The major organizations developing standards in the mobility industry are based in the United States, Europe, China, and Japan.

In AC distribution systems, most standards are well established and widely accepted. Even though the DC microgrid topic area has been studied over the years for its advantages, DC power distribution for EV charging is still an emerging technology. This sector faces challenges related to void standardized regulations and innovation gaps. Thus, for realization of this technology in EV applications, there is a need to adapt standards and practices of similar power and voltage levels established in other applications [31]. Considering the advantages of the DC distribution system, standardization efforts are found for different industry areas including data centers, buildings, PV applications, offshore DC wind power collection, DC power distribution in rail, and on-board marine DC microgrid. Some aspects of EV charging infrastructure of various power and voltage ratings are also addressed within some of the standardization efforts of the International Electrotechnical Commission (IEC), Institute of Electrical and Electronics Engineers (IEEE) Standards Association, EMerge Alliance [32], Current OS [33], and other organizations.

There are several examples of established DC distribution systems in other industries in the voltage range of 24 V to 1,500 V. Some other applications of higher voltage levels can also be taken into consideration for the adapted analytical methods and lessons around protection and electromagnetic interference (EMI). Residential buildings, certain industrial installations, data centers, and stationary auxiliary power systems have substantial advantages when a DC distribution system is adapted. Higher efficiency, resiliency, and easier integration drive several standardization efforts in these applications. The European Telecommunications Standards Institute's standard, ETSI EN 300 132-3-1, discusses low-voltage direct current (LVDC) systems of up to 400 V and is mainly designed for telecommunications and data center equipment [34]. It also takes protection, grounding, and electromagnetic compatibility (EMC) related requirements into account. The EMerge Alliance is an open industry association with the vision of deploying advanced architectures and control systems based on DC microgrids, with a specific focus on data and telecommunication centers, occupied spaces, and buildings [32]. The IEC SG4 standard covers 1,500 V DC distribution [35]. It is the only standard with a focus area related to EVs, along with data centers, energy storage systems, and commercial buildings. The aspects of grounding, redundancy, topology, etc. can be adapted from the aforementioned standards into the DC hub development effort.

DC distribution systems in shipboard and marine applications are another source of reference for adaptation. Electrified DC and hybrid ship power distribution systems have several advantages in terms of size, weight, volume, efficiency, manpower requirements, and ease of ESS integration. The maritime industry has adapted to the DC power distribution system and established standards around their applications. Military standard MIL-STD-1399 includes sections defining the requirements of DC equipment in shipboard power systems [36]. The U.S. Navy program Naval Sea Systems Command (NAVSEA) has been addressing medium voltage direct current (MVDC) standards for surface ship applications as an additional supplement to its standards [37]. IEEE Standard 1709 provides guidelines to specify, procure, design, manufacture, and develop manuals, safety procedures, practices, and procedures for effective maintenance of MVDC electrical power systems [38].

With the adaptation of high-power rated DC switch gears in different voltage ranges, the railway industry's traction systems have always been a prime example for success in DC power distribution systems. Standards and practices around railway infrastructures also provide valuable references for the development of DC distribution systems for EV applications. The electrification system ranges from 600 V to 9 kV. The permissible range of voltages allowed are as stated in EVS-EN 50163 [39] by the Estonian Centre for Standardisation and Accreditation and in IEC 60850 [40]. The British Standards Institution published BS EN 50367 to define the criteria for technical compatibility between pantographs and overhead contact lines to achieve access to European railway networks [41]. IEC 62128-1 addresses railway applications for electrical safety, earthing and protection against shock for both AC

and DC traction systems [42]. Referring to these standards for railway application, we can derive various essential aspects that would aid in the development of a DC Hub for eCHIP.

In addition to the above mentioned standards, concepts from IEEE 1547 on aspects of interconnection and safety considerations for distributed energy resources are adaptable for our use case as well [43]. Thus, for DC hub development in the eCHIP project, several aspects from prevailing standards and practices can be referenced.

2.5 DC-Hub Communication Protocols/Standards Overview

The DC hub has the potential to utilize multiple communication protocols and standards for integrating devices into its SEMS. The SEMS must be capable of communicating with any device to conduct metering, monitoring, and control functions. Currently, there is a lack of industry consensus on what communication protocol to use for specific devices. The choice of protocol for this project will depend on several factors, such as application/device specifications, data transfer requirements, desired security levels, and budget constraints. To create a fully integrated SEMS, it may be necessary to combine multiple protocols. The following communication protocols are not a fully exhaustive list but include some of the most prevalent protocols utilized in the current SEMS, and even buildings, similar to the goals of this project.

2.5.1 Open Charge Point Protocol

For EV charging infrastructure, the de-facto standard for communication is the Open Charge Point Protocol (OCPP) [44]. The OCPP protocol is an open standard that allows monitoring, configuration, and management of EV charging stations. It uses a client-server model where the charging station is the client and a charge station management system (CSMS) or charge point operator is the server. The protocol is designed to be extensible and has a defined set of messages that can be expanded to support additional functionality. The protocol defines operations that can be performed on a charging station, such as starting and stopping a charging session, querying the station's status, and updating firmware. These operations are performed using defined messages exchanged between the charging station and the CSMS. OCPP 1.6 supports both Simple Object Access Protocol (SOAP)/XML and JavaScript Object Notation (JSON)-RPC encoding formats for interoperability with various programming languages and platforms. It also has security features like message signing and encryption to ensure privacy and integrity of communications.

A key benefit of OCPP is its ability to support interoperability between different EV charging station manufacturers and network operators. By using this standardized protocol, a CPO can integrate any OCPP-supported charging station regardless of manufacturer. This promotes competition and innovation in the EV charging industry while providing a consistent user experience for EV drivers.

OCPP is an important standard for the EV charging industry that provides a flexible and extensible protocol for managing charging stations while promoting interoperability between different manufacturers and network operators. Typical deployments by charge station operators would include a cloud-based CSMS serving a large number of spatially diverse stations. However, it is becoming increasingly common for charge station operators to deploy a local OCPP-based CSMS for local monitoring and control of EV charging infrastructure. The vast majority of deployments are the OCPP 1.6J protocol. However, this protocol has been updated (OCPP 2.0.1) to increase security, diagnostics, and the ability to handle the International Organization for Standardization (ISO)'s ISO-15118 [45] messages/use-cases including smart charge scheduling.

2.5.2 Modbus

Modbus is a communication protocol that has become popular in industrial automation and control systems [46]. Its flexibility, interoperability, and ease of use have made it a versatile and robust protocol. It provides a reliable and cost-effective solution for communication between devices such as sensors, actuators, and programmable logic controllers using various communication media like serial lines, Ethernet, and wireless networks.

The protocol follows a controller-peripheral architecture for smooth and efficient communication between devices. The controller device sends a request to the peripheral device, which responds with a message containing the requested data. Modbus supports multiple function codes that define the type of request being made, such as reading or writing data or controlling a device. It also has error-checking and recovery mechanisms for accurate and dependable communication.

Modbus has diverse variants including Modbus RTU, Modbus ASCII, and Modbus TCP/IP. Modbus RTU and Modbus ASCII use serial communication, while Modbus TCP/IP uses Ethernet. Modbus RTU and ASCII are used in legacy systems, while TCP/IP is gaining popularity due to its support for modern networks.

2.5.3 BACnet

BACnet is an open communication protocol widely used in building automation and control. In 1995, it was recognized as an American National Standards Institute standard, and later in 2003, it became an ISO standard [47].

BACnet provides a standardized way for devices such as sensors, actuators, and controllers to communicate with each other and with higher-level systems like building management systems. BACnet uses a client-server architecture where clients initiate requests to servers, which respond with data or perform control actions.

The protocol supports several communication media, including Ethernet, ARCNET, and LonTalk. It also includes standard object types like analog inputs, binary inputs, and schedules that represent common building automation and control functions. BACnet uses standard services like read, write, and subscribe to interact with these objects. It also supports alarms, trends, and schedules for advanced automation and control applications. BACnet is mature and widely adopted, with support from many vendors and organizations. Its open nature and standardization make it popular for building automation and control systems, as it allows interoperability between different devices and systems. However, its complexity and flexibility can present challenges for implementation and deployment.

2.5.4 Message Queuing Telemetry Transport (MQTT)

MQTT is a messaging protocol that was created for situations where network bandwidth and device resources are limited. It is an OASIS standard [48]. The protocol operates on a publish/subscribe model where clients publish messages to topics and other clients subscribe to those topics to receive the messages.

This allows for efficient communication between many clients, since each client only needs to subscribe to the topics it is interested in. An MQTT broker acts as an intermediary between publisher and subscribers. The broker receives messages from publishers, delivers them to subscribers, manages subscriptions, and ensures that messages are delivered according to the requested quality-of-service (QoS) level. MQTT is designed for use with unreliable or intermittent network connections and has features such as message persistence and QoS levels to ensure message delivery. The QoS levels range from 0 (least reliable) to 2 (most reliable), with increasing overhead.

MQTT is commonly used in internet of things (IoT) and machine-to-machine applications for transmitting data between devices and applications. It is supported by many programming languages and platforms and has become popular due to its lightweight nature and ability to operate over unreliable networks.

2.5.5 Open Field Message Bus (OpenFMB)

The OpenFMB is an interoperability framework that was ratified as a standard in 2016 [49]. The OpenFMB framework is an architecture that facilitates device-to-grid communication rather than just a communication protocol. OpenFMB uses a publish/subscribe messaging model for real-time communication between devices and systems in the electric power grid. Its vendor-agnostic design allows for integration of a wide range of devices and applications.

The OpenFMB framework uses various communication protocols and standards for seamless communication between devices. These protocols include the Common Information Model or CIM, [50], IEC 61850 [51], Distributed Network Protocol 3 or DNP3 [52], and MQTT, among others, to ensure efficient and secure data exchange. OpenFMB enables the development of distributed energy resource management systems (DERMS) that can integrate and control sources like solar panels, ESS, and EVs. It also enables the creation of microgrids, which are small-scale power grids that can operate independently from the main grid.

OpenFMB is a promising standard for integrating and controlling distributed energy resources in the electric power grid. Its vendor-agnostic architecture and support for existing protocols make it flexible and adaptable for various applications.

2.5.6 Open Automated Demand Response (OpenADR)

OpenADR is an open, standardized communication protocol for demand response (DR) management [53]. It allows utilities and grid operators to send signals to commercial, industrial, and residential customers to reduce their electricity consumption during peak periods or other times of high demand. It is designed to be vendor-neutral and interoperable, allowing utilities and customers to use different hardware and software solutions.

By integrating OpenADR into an energy management system, the operator can receive signals from the grid operator to reduce energy consumption during peak demand periods. OpenADR can also be used to participate in price-based DR programs, where the utility provides pricing signals to the hub based on the current market price of electricity. The energy management system of the hub can use these signals to adjust energy consumption and charge or discharge the battery to take advantage of lower electricity prices.

OpenADR allows systems to participate in DR programs and optimize their energy consumption based on the needs of the grid and the availability of renewable energy sources. This can help reduce the hub's overall energy consumption and its impact on the grid while reducing costs and improving grid reliability. OpenADR has the potential to be used to integrate the charging facility experiment that will be developed under the scope of this work with the grid.

3 Architecture and Design Parameters of the Selected DC Charging Hub

3.1 Parameter Specification and Device Selection for the DC Hub Power Architecture

The selected architecture for the DC charging hub testbed with all the available and proposed components is shown in Figure 7. While this figure includes the overall diagram for the DC charging hub, it is not limiting the scope of the component types, the number of nodes that can be connected to the hub, or the voltage/power ratings of the components. For most of the components described in the figure, there is more than one commercial off-the-shelf (COTS) product option available to develop use cases at different power levels in a phased manner. Also, the configuration, voltage, and power levels will change depending on the components being evaluated. The testbed shown in Figure 7 is configured at NREL's Energy Systems Integration Facility (ESIF).

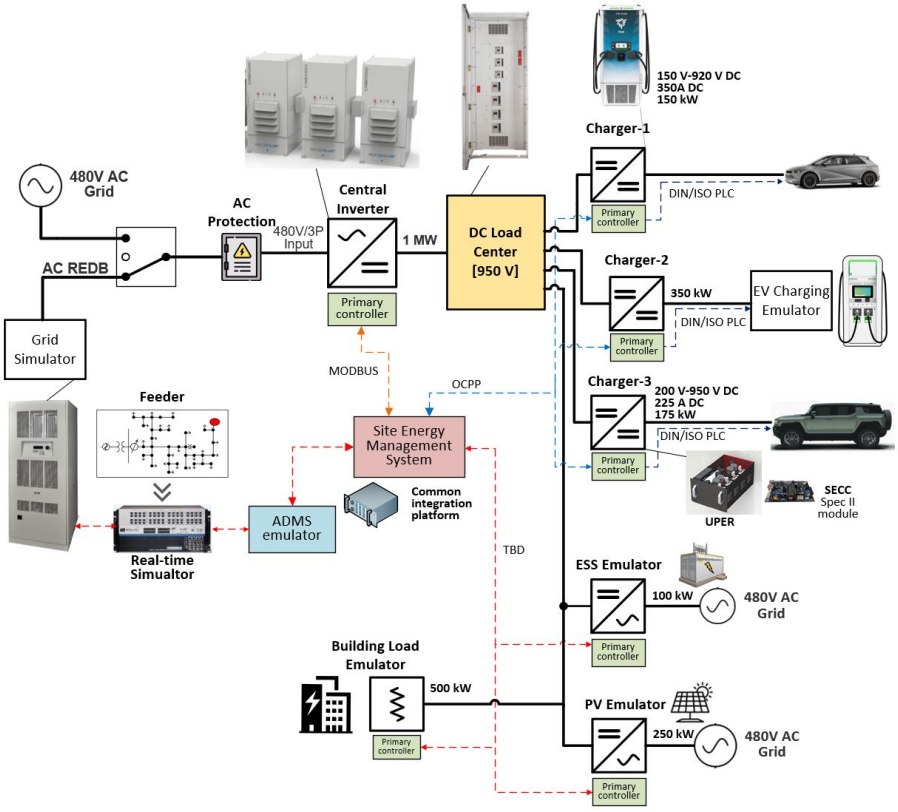

Figure 7. DC charging hub experimental testbed

3.1.1 Inverter Selection

A COTS bidirectional inverter is fed by a 480-V, three-phase, AC grid source. There are two COTS inverter options available that will be used for the project within ESIF at NREL. The parameters of the inverters are listed in Table 2. The primary tests that focus on implementing the first version of the SEMS control algorithm are performed using the Anderson AC2660P. Therefore, the initial tests are focused on functionality rather than operating at the rated power. On the other hand, the EPC Power CAB1000 will enable advanced grid integration use cases such as V2X, grid islanding, and reactive power support during the upcoming phases of the project. It will also provide a higher power-rated experimental platform.

3.1.2 DC Bus Selection

The inverter connects to a DC bus called the DC Research Electrical Distribution Bus (DC-REDB) at NREL's ESIF. DC-REDB runs through different labs within ESIF connecting different DC resources. The DC-REDB is a three-

Table 2. Inverters Used in the DC Hub

	Inverter type	
Parameter	**Anderson AC2660P**	**EPC Power CAB1000**
AC Voltage	480 V, three-phase	480 V, three-phase
DC Voltage	265 V–1,000 V	720 V–1,250 V
Power Rating	660 kW	1,043 kW
Communication	Fiber-optic Modbus TCP — CAN	— Modbus TCP/IP Modbus RTU CAN

wire (positive, negative, ground) system with three-pole switches and rated for maximum voltage of 1,000 V DC. The length of the bus can be a few hundred feet long depending on the configuration used during the test.

As a vital node connecting various DC resources within the research facility, DC-REDB requires comprehensive protection to ensure its safe and reliable operation. Proper protection measures are essential to prevent potential hazards and system failures. To enhance the safety and reliability of the DC hub, redundant protection devices are employed throughout the system. Each source connected to the DC hub is equipped with a REDB connection device (RCD) or mobile RCD (MRCD). These RCDs and MRCDs are designed to provide emergency-power-off functionality and overcurrent protection, ensuring that any abnormal conditions can be rapidly isolated to prevent damage to the system and connected devices.

DC switches, typically sourced from manufacturers such as Sécheron, Eaton, and ABB, are specifically selected to meet the requirements of the DC-REDB. These switches are designed to open or close only when the voltage is less than 135 V, providing an additional layer of safety during operations.

In order to maintain a reliable and secure connection between different resources within the DC-REDB, P3-type connectors are exclusively used for wire connections. The use of these specialized connectors ensures proper alignment and minimizes the risk of accidental disconnections or unsafe conditions.

Additionally, a DC load center (DC LC) (as shown in Figure 7) is under development as an alternative to DC-REDB and will have the ability to be connected to DC-REDB. It could also be directly fed by the COTS inverter and establish its own DC distribution. DC LC has a bipolar configuration, and it will be sited outdoors with the National Electrical Manufacturers Association's NEMA 3R rating. It will serve the DC hub nodes (i.e., EV chargers, distributed energy resources, other loads) while providing protection, monitoring, and switching on each circuit. The DC LC will be rated at 2,000 V to provide connection to future HPC equipment.

3.1.3 COTS DC-DC Charger

A COTS Tritium PKM150 DC-DC charger is used for the project. The EVSE unit is capable of simultaneously charging up to two EVs with an aggregate charging power of 150 kW. The two plug-in connectors are CCS and CHAdeMO with maximum ratings of 350 A/920 V DC and 125 A/500 V DC, respectively. Tritium PKM150 allows separate control of charging power per each charging port via OCPP v1.6J. The nominal input voltage rating of the EVSE is 950 V. Within the scope of the project, there will be additional COTS DC-DC chargers that will be acquired and will be integrated to the above-mentioned DC bus. The primary results and functionality tests are performed using Tritium PKM150.

3.1.4 Battery Energy Storage System Emulation

A battery ESS is realized and connected to the DC hub as shown in Figure 7. The ESS model is simulated on an OPAL-RT 5700 real-time machine. The OPAL device communicates with a bidirectional DC/AC inverter for real-time battery emulation. For this purpose, a 100-kW bidirectional DC-AC converter, NHR 9300, is used. It is rated at 1,200 V DC and 167 A DC.

3.1.5 PV Emulation

A Magna-Power MTA1000-250 MT Series VI DC power supply is used to emulate PV generation. This DC power supply emulates a PV array connected to the DC hub via a DC-DC converter. The supply is rated at 250 kW, 1,000 V DC, and 250 A DC. The DC power supply is effectively a unidirectional DC-AC converter, through which power

sourced from the laboratory 480 V AC house power is supplied to the DC hub. The DC output port of the supply is connected to the DC hub via fixed-equipment switch board (FESB) containing protection devices. The DC power supply is operated in current-control mode. To emulate PV generation, the SEMS platform sends current commands to the DC power supply at a frequency of 1 Hz. The communication uses the Standard Commands for Programmable Instruments (SCPI) protocol over TCP/IP. To capture the higher-frequency variability of PV generation, a PV power profile is generated from 1-second resolution PV data from [54]. These power values are measured at the DC-side port of the PV array's inverter, and therefore include the dynamics of irradiance variability and MPPT tracking. To generate the current command to the DC supply, the SEMS platform divides each power setpoint from the PV profile by the measured DC bus voltage.

3.1.6 Building Load Emulation

A Simplex Mars DC load bank is used to emulate a site or building load. The load bank comprises a bank of switchable resistive elements, which dissipate power as heat. The load bank is rated at 505.5 kW, 1,000 V DC, and 505.5 A DC. Due to the discrete resistive elements, the resolution of the controllable load is limited to 0.5 kW. The load bank is connected to the DC hub via a tap-box (direct connection). To emulate a building load, the SEMS sends control commands to the load bank at a frequency of 1 Hz. The communication uses the Modbus protocol over TCP/IP. A building load profile is generated from 1-second resolution building load data from [55]. The power values are measured directly from the electrical cabinet of an office environment. Since the load bank is controlled by switching the individual resistive elements, the SEMS platform converts each power setpoint from the load profile into the set of resistive elements/load steps to turn on in the load bank.

3.1.7 Electric Vehicles

Two market EVs are used for the initial phase of the study: Hyundai Ioniq 5 and Nissan Leaf. The Ioniq 5 has a nominal pack voltage of 800 V with a maximum charging power capability of 235 kW. The Leaf has a nominal pack voltage of 348 V and a maximum of 40 kW charging power. Future phases of the project will include other new market EVs such as the GMC Hummer EV and Ford F-150 Lightning. Figure 8 shows the two EVs charging side by side, fed by the Tritium PKM150.

Figure 8. EV charging setup for concurrent charging via CCS (Ioniq 5) and CHAdeMO (Leaf) provided by the Tritium PKM150 at NREL's ESIF

The DC charging hub testbed also incorporates a custom-built EV charging emulator, as shown in Figure 7. This can emulate a particular vehicle or any desired charging behavior. From a charger's perspective, the EV charging emulator appears identical to a real vehicle. However, the charging power is being fed back to the utility connection rather than an EV and its battery. This increases the versatility of the test platform. Additionally, the testing is more efficient, since the emulated vehicle can be charged continuously and there is no need to discharge the battery, as is the case when testing a real vehicle. The EV emulator can realize pack voltages up to 1,000 V DC and up to a charging power of 500 kW.

3.2 ORNL-Developed DC-DC Charger Topology and Parameter Specification

In this project, a DAB topology has been selected for the DC-DC charger implementation. The isolated DC-DC DAB converter is referred to here as a Universal Power Electronics Regulator (UPER), interfacing the DC distribu-

tion bus and the vehicle. The intent is to build a 1,000-V, 175-kW charger that could serve as a module that can be scaled up for higher power requirements. The design specifications of the 1000-V class charger are listed in Table 3.

Table 3. UPER Specifications

Parameter	1000-V Class UPER
Output power	175 kW (scalable to 0.5 MW)
Input Voltage	900 V $+/-5\%$
Output Voltage	580 V–860 V at rated current 290 V–380 V at rated current 250 V–900 V at 50 A max
Rated Output Current	200 A
Power flow Efficiency	Bidirectional $>99\%$
Operating Temperature	TBD to 40°C
Module Dimensions	24" h×36" w×25" d
Enclosure Dimensions	60" h×36" w×25" d
Cooling	Forced air
Vehicle Connector	CCS Type2 (can be modified)
EV Comm. Protocols	DIN 70121 and ISO-15118
Control Power	110 V AC, 10 A

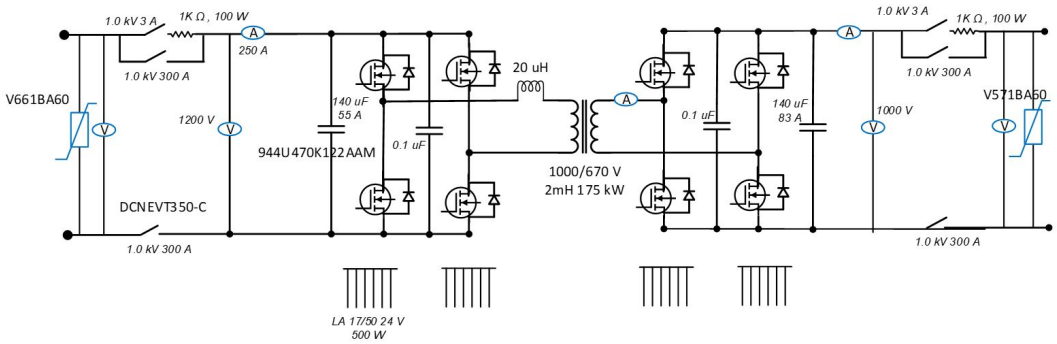

Figure 9. 1000-V class charger schematic

The detailed design schematic of the 1000-V class charger is shown in Figure 9. The charger is based on 1.7-kV, 350-A SiC MOSFETs. The switching frequency has been chosen to be 20 kHz to reduce the acoustic noise. The transformer turns ratio has been selected to limit the voltage variation to be within +/- 15% of nominal voltage while the vehicle is being charged. The bill of materials (BOM) of the 1,000-V class charger is shown in Table 4.

It was identified that achieving a wide voltage range (250–950 V) using a DAB-based charger is a key technical challenge. The proposed DAB DC-DC charger achieves ZVS over wide current and voltage range by implementing passive and active techniques. The passive technique involves adding a tap on the secondary side of the medium frequency transformer, as shown in Figure10. The tap is used to provide correct voltage to either a 400-V class vehicle or an 800-V class vehicle. The proposed active method is a novel zero state modulation (ZSM) technique that will be implemented at lower currents and nonunity voltage ratios. The ZSM method allows ZVS operation at lower currents and for nonunity voltage ratios. In the high current range, the standard single phase modulation (SPM) technique will be implemented, as this will result in ZVS, high efficiency, and low root-mean-square (RMS) current operation. Figure 11 shows the experimental design pictures for the UPER DC-DC converter and scaled-up HPC rendering.

3.3 ANL-Developed SpEC Module Integration Specifications

The Smartgrid EV Communication (SpEC) module developed by Argonne is a smart EV communication controller that enables DC fast charging communication between an EV and the charger. The SpEC module acts as the supply

Table 4. 1000-V class Charger BOM

Item	Part No.	Quantity
1700 V, 280 A, 5.8 mΩ, SiC devices	MSCSM170AM058CT6LIAG	4
1.7 kV gate drives	Custom	8
Film caps 1400 V, 100 μF	944U470K122AAM	2
Film caps 1400 V, 0.47 μF		4
LEM current sensor, 300 A	LF 310-s	2
Voltage sensor, 1000 V	ORNL sensor	2
Transformer, 20 kHz 175 kW	Custom	1
Inductor, 15 μH	Custom	1
Heatsink	LA 17/100	4
Contactor 900 V, 10 A	DCNEVT350-C	2
Contactor 900 V, 300 A	DCNEVT350-C	2

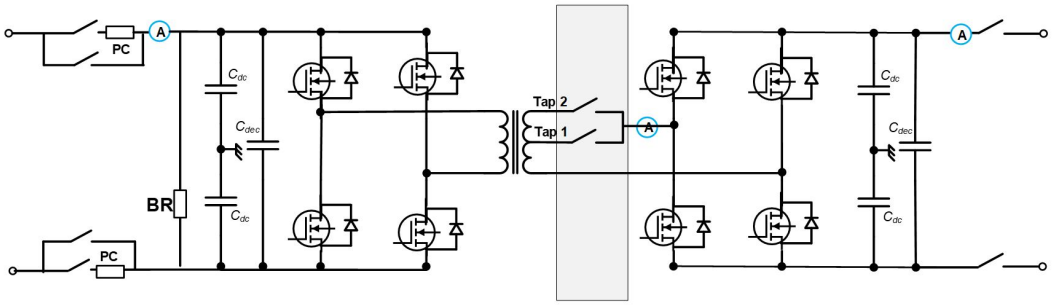

Figure 10. Proposed taps to select between 400 V class and 800 V class vehicles

equipment communications controller (SECC); and the UPER, along with the SpEC module, collectively behave as the EVSE. These two modules have tight integration between them to allow reliable communication between the power electronics and the EV. A block diagram of the EVSE comprising of SpEC and UPER is shown in Figure 12.

Three key components for successful UPER-Spec integration in the eCHIP project are (1) hardware and firmware development of the SECC, (2) developing a communication protocol between the SECC and UPER, and (3) designing and developing the software architecture as well as main applications for the SEMS, which will be explained in detail in Section 4.

The SpEC module implements high-level communication required for DC charging based on DIN SPEC 70121 and ISO 15118 standards. The SpEC module is the interface between the EV and EVSE, and the communication between them is via power line communication (PLC) over the CCS connector's control pilot line. The SpEC module will translate the XML/EXI messages to and from the EV, as well as accept commands from the SEMS.

ANL researchers will use both the Gen I and Gen II SpEC modules (Figure 13) in the development and demonstration phases of the project. Leveraging the DIN 70121 stack, researchers will update the firmware to implement the ISO 15118-20 standard to accomplish bidirectional DC charging. Custom firmware will be written to interface with the UPER and the SEMS.

The SpEC and UPER will communicate with each other using the controller area network (CAN) bus protocol. The CAN bus is specifically designed to be a communication protocol for automotive applications, where a vehicle may have several electronic control units for various subsystems.

3.4 DC Hub Communication System Design and Requirements

The DC-DC EVSE based on the UPER and SpEC module will integrate with the SEMS platform via a combination of OCPP and MQTT. OCPP will be used to handle monitoring and control of EV charging, while MQTT will be used to implement nonstandardized DC hub integration monitoring and control. The SpEC module will handle all the SEMS communication for the EVSE, along with communicating with the vehicle. An overview of the EV-

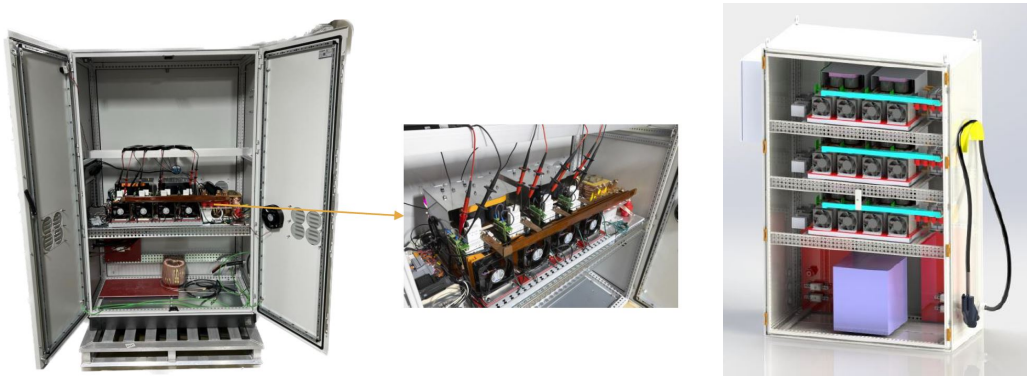

(a) UPER 1000 V, 175 kW module experimental picture

(b) UPER scaled-up, higher power charger rendering figure

Figure 11. UPER charger design pictures

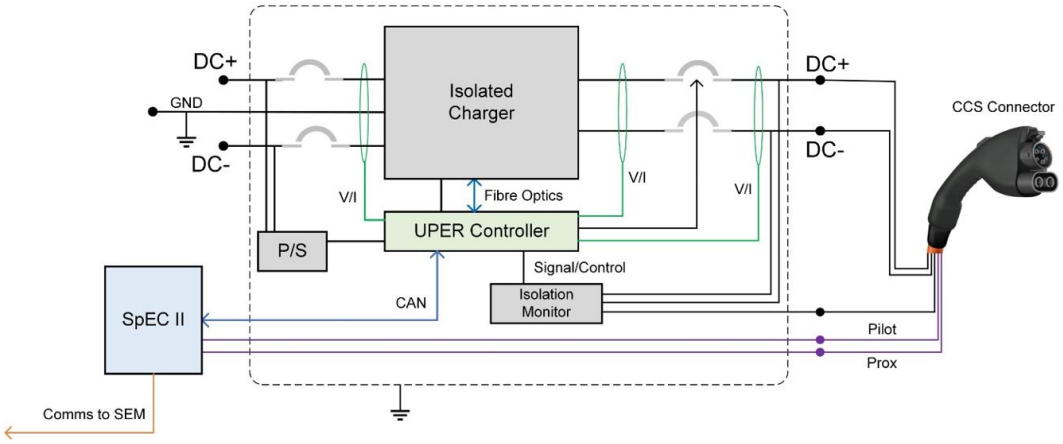

Figure 12. Block-diagram of the EVSE with UPER and SpEC integration

charging-related communication protocols that are planned to be implemented in this project are shown in Figure 14. The selection of protocols shown is not final and is subject to change.

3.4.1 OCPP Implementation at eCHIP

As of 2023, most OCPP-based charging stations have been deployed with OCPP 1.6J (2015), which uses WebSockets and JSON payloads to communicate between the EVSE (charging station) and the central server (also known as a CSMS). OCPP 2.0.1 is the latest major release of the OCPP protocol, which incorporates ISO 15118 messages that enable plug and charge as well as charge scheduling. Since OCPP 2.0.1 has several breaking changes over previous versions, the core profile as outlined in the OCPP 1.6J protocol will be deployed for initial testing of the UPER/SpEC charger and will be updated to OCPP 2.0.1 when ready.

Optimized charge scheduling that prioritizes the travel needs of the EV driver and the power constraints of the local grid is possible using ISO 15118 and OCPP 2.0.1. It enables dynamic demand response based on the grid's demand, load balancing that adjusts the charging rate based on grid capacity, and prioritized charging for EVs that need it most. Other applications include grid frequency regulation and vehicle-to-grid (V2G) capabilities where EVs can provide energy back to the grid during periods of high demand. V2G services may be opt-in programs where EV owners can earn credit by selling their excess energy back to the grid and ensuring that other charging EVs get the highest power available for a charge session.

Figure 13. SpEC module Gen I (left) and Gen II (right)

Figure 14. EV charging communication protocols that are being implemented at eCHIP

A charge scheduler application/logic must be added to the OCPP 2.0.1 CSMS to receive the maximum power profiles from the grid operator. The charge scheduler must handle initial charge schedules, initiate renegotiations, and handle EV-initiated renegotiations. A successfully negotiated charge schedule meets the needs of the EV driver, while the aggregate charge schedules of all EVs managed by the charge scheduler do not exceed the maximum power profile provided by the grid operator.

3.4.2 MQTT Implementation at eCHIP

In this project, an MQTT broker will be deployed within the SEMS to facilitate customized communication between local controllers and the SpEC module, which in turn communicates with the UPER DC-DC charger via CAN. Customized controls such as ramp rate and droop control will be implemented utilizing the MQTT protocol. The specific topics and payload format will be defined as the use cases are identified.

3.4.3 Other DC Hub Communication Protocols Implemented at eCHIP

The SEMS deployed for the eCHIP project must be able to interface with other TCP/IP based protocols such as Modbus and BACnet. Devices such as AC/DC meters and solar inverters typically deploy a Modbus TCP/IP interface. In addition to device-to-system protocols, the SEMS must be able to communicate with a grid operator. For the eCHIP project, OpenADR will be used to communicate to a grid operator's DERMS.

4 Site Energy Management System (SEMS)

SEMS refers to monitoring, controlling, and optimizing energy usage in a DC charging hub. SEMS involves the implementation of strategies aimed at reducing energy consumption, increasing efficiency, minimizing costs, and defining interactions between hub components. This section details the common SEMS objectives, introduces available SEMS architectures and performance metrics, discusses the real-time implementation methods via current standards.

4.1 Background and Objective Definition

Some of the common objectives of an SEMS strategy, along with their implementation challenges and requirements, are detailed below. Note that this work is still in progress, and the below list does not exhaustively describe all the available application use cases. Those that are not listed below may include V2X, grid islanding, and emergency use cases.

4.1.1 Optimizing Charging Time

The charging time optimization objective refers to the goal of reducing the time it takes to charge an EV battery. The shorter the charging time, the more convenient it is for EV owners, and the more likely they are to adopt and use EVs. This objective is often constrained by the rated charging power of the DC-DC converter, the maximum charging power requested by an EV battery management system (BMS), and the total amount of power that is available within the charging hub.

4.1.2 Optimizing Charging Cost

The charging cost minimization objective aims to reduce the cost of charging EVs for both the EV owners and charging station operators. However, this objective comes with potential challenges and requirements. One major challenge is the need for a flexible pricing structure that considers the cost of electricity, the time of day, and the demand for charging stations. Additionally, the integration of renewable energy sources (such as PV) and ESS into the charging infrastructure can help to further reduce costs.

4.1.3 Optimizing Load- and Energy-Sharing

Load- and energy-sharing optimization for a DC charging hub aims to reduce the operational costs associated with running high-power chargers, ESS, distributed energy sources (e.g., PV), and other loads in tandem. This objective can be achieved by optimizing the use of energy through energy sharing. The typical approach is to use power from the electric grid to operate high-power chargers and charge ESS when energy prices are low. The stored energy is then used during periods when energy prices are high. This operation can be further optimized in the presence of distributed energy resources. This approach requires high coordination and information flow between units.

4.2 Architecture and Design Parameters for the SEMS

The above objectives can be achieved by using different high-level SEMS architectures that have unique advantages and disadvantages. This section first defines several SEMS metrics to better evaluate the performance of a given architecture and then introduces common SEMS architectures that could be used in DC charging hubs with their requirements.

4.2.1 SEMS Performance Metrics

4.2.1.1 Scalability and Modularity

Scalability refers to the hub's ability to expand or contract its capacity as needed. Since the demand for power can vary over time, the DC hub should be able to accommodate load changes without compromising its stability or efficiency. A scalable SEMS architecture should add or remove components, such as high-power chargers or ESS, to adjust its capacity as needed.

Modularity refers to the ability of the hub components to be easily interconnected and interchanged. This means that the hub can be built and expanded in a modular fashion with the help of an SEMS. A modular charging hub is easier to design, install, and maintain than a nonmodular one, because the components can be standardized and easily replaced as necessary.

4.2.1.2 Resiliency

Resiliency is a critical characteristic of an SEMS, as it ensures that the system can continue to function reliably and provide power to critical loads in the event of disturbances or disruptions. Incorporating renewables and ESS into an SEMS can provide a decentralized source that can continue to provide power during grid outages. This approach also improves the overall reliability of the system by reducing dependence on a single power source. The SEMS can be designed to prioritize critical loads and reduce power to noncritical loads during disruptions. This allows the system to maintain power to essential equipment and services, even if the total power supply is reduced.

4.2.1.3 Optimality

Optimality is an important characteristic of an SEMS, as it ensures that the system operates as effectively as possible while still meeting the desired performance goals. Accurate forecasting of power demand and generation allows the SEMS to schedule the use of energy resources optimally. The SEMS can balance the loads across different energy resources to ensure that they are used in an optimal manner. The SEMS can participate in demand response programs, which incentivizes consumers to reduce their consumption during periods of high demand. Real-time monitoring and control are also critical for an optimal SEMS to quickly respond to changes in demand or supply.

4.2.1.4 Stability

Stability is the ability of the SEMS to ensure that the system can operate safely and reliably without any major disruptions or failures. More specifically, stability in a DC hub refers to the DC bus voltage stability. Accurate modeling and analysis of the DC hub can help identify potential stability issues and ensure that the SEMS is designed to operate within safe operating limits. The SEMS should have a control and regulation mechanism to stabilize the DC voltage in the face of disturbances and disruptions.

4.2.1.5 Communication Dependency

Communication dependency refers to the degree to which the SEMS relies on communication networks to transmit information between different components and subsystems. Effective communication ensures that all components of the SEMS can share real-time information on power demand and supply, system status, and potential problems, and to coordinate their actions to optimize system performance. Although enhanced information flow enables the development of more advanced and efficient SEMS control strategies, this high communication dependency also renders the SEMS vulnerable to networking failures and cyberattacks, which reduces the system's resiliency.

4.2.1.6 Computational Complexity

Computational complexity refers to all the resources required to implement the SEMS controller. Some SEMS architectures depend on heavy computations such as solving multi-objective optimization problems with hundreds of variables and constraints or differential equations, whereas others use only light calculations. The hardware is therefore critical to determine the minimum step time of the SEMS controller. The availability of robust solver libraries, fast data processing, accurate real-time measurement, and stable communication networks will affect the SEMS controller's computational needs.

4.2.2 SEMS Controller Architecture

SEMS controller architecture defines how the SEMS will be implemented based on the desired objectives and interaction capabilities within the DC hub. Some common architectures are discussed below, along with advantages and limitations.

4.2.2.1 Centralized Control

In a centralized controller architecture, a single entity or controller is responsible for managing and directing the operations of a system through a dedicated communication network and protocols. The centralized controller typically uses a combination of power, voltage, and current measurements to monitor the energy flow and sharing between different DC hub components. The controller may also receive inputs and signals from customers (e.g., departure time, energy demand, willingness to participate in smart charging, state of charge, BMS response), the hub operator (e.g., cost minimization, peak demand reduction), and the utility grid (e.g., price signal, grid support need). With the input parameters and measurements collected on the server computer, the SEMS controller computes and dispatches power set-points to each hub component through OCPP and other communication protocols discussed before. Calculation of power set-points could be as simple as using heuristic rules or as complex as formulating a multi-objective optimization problem with customers and operator constraints to achieve certain previously described objectives. The main advantage of a centralized architecture is that the operation can be optimized to achieve high operational efficiency due to real-time monitoring, accessing, and control. However, this architecture can also introduce a single

point of failure, as the entire system may be disrupted if the central controller fails or becomes overwhelmed, or the communication system collapses. Additionally, the centralized controller may become a performance bottleneck if it is unable to handle the demands of the system. This characteristic of the centralized architecture increases resiliency concerns and reduces the system's ability to easily scale.

4.2.2.2 Decentralized Control

The decentralized controller architecture is an approach that distributes control and decision-making across multiple devices in a hub. Rather than relying on a single centralized controller to manage all energy-related functions, a decentralized architecture allows for more flexible and dynamic control of energy usage that can lead to plug-and-play operation and increased scalability. A critical advantage of the decentralized approach is that there is no real-time communication requirement to operate. The preset controller rules and actions can be hard-coded into the devices connected to the hub. Since there is no central controller to compute the power set-points, the individual hub components compute their input/output power set-points based on local information, which is usually the DC hub voltage. The traditional droop controller is a good example of a decentralized scheme where the power-set points are piecewise linear functions of the bus voltage. Once the parameters of the droop functions (rules) are properly defined, the hub units operate by monitoring only the bus voltage (i.e., communication-free). The CurrentOS protocol [33] also offers a similar decentralized approach where the bus voltage is divided into discrete bands to inform the units about the power availability within the system and to make them react accordingly. The main drawback of the decentralized approach is that the overall performance and operational efficiency highly depends on the shape and parameters of the rule functions. Therefore, the rule parameters need to be properly tuned based on the system-level objectives.

4.2.2.3 Adaptive and Distributed Control

A centralized controller is vulnerable to single-point and communication failures, despite offering optimal operation. A decentralized approach, on the other hand, is more resilient and scalable; however, its performance might be suboptimal due to poor parameter tuning. A compromise can offer the best of both worlds by enhancing the resiliency and scalability while increasing the operational optimality. This may be achieved by using a decentralized approach in conjunction with a communication capability that is in between individual units and a central server. This is known as distributed architecture. In this setup, the bus components may communicate and receive information as needed and adaptively update their controller rules. Real-time connectivity is optional, but irregular information exchange may be needed to drive the operating point close to optimal. The final power set-points are still determined at the individual units. This architecture can take advantage of the available communication network to improve the operational efficiency while also operating when a network failure occurs. The parameters of the decentralized droop control, for example, can be retuned *ad hoc* to adapt to the changing hub conditions (i.e., PV generation, price signal, customer demand). In the case of a network failure, however, the units will still continue to operate with their set parameters.

4.2.3 SEMS Specifications and Requirements

There are several criteria determining the SEMS control specifications. These are usually tied to the desired SEMS objectives and performance metrics. The SEMS architecture is then selected based on these requirements. For instance, if an optimal site operation is required where the power flow is optimized based on cost or charging time, the hub components must be updated in real time with the new power set-points generated by a central controller. This way, the hub can be operated optimally in exchange for high communication dependency, computational intensity, less scalability, and reduced resiliency. If, on the other hand, resiliency and scalability have higher priority in the hub operation, a decentralized or distributed approach can sacrifice some efficiency in the hub operation but gain more plug-and-play flexibility. Some hybrid solutions and scenarios can also be possible, depending on special use cases.

There is no best SEMS strategy or specifications that can fit to all use cases and hub architectures. The availability of reliable communication networks and computational resources are highly determinant. The specifications and characteristics of an individual hub's components also play a critical role. A droop type of control, for example, can only be implemented if the controllers of individual converters can be configured to follow a droop function. Another factor affecting the specifications of a high-level SEMS controller is the response time of high-power chargers and EVs. A SEMS controller should not operate (i.e., generate power set-points) faster than the converter or BMS with the slowest response. This requires experimental analysis and testing to extract the relative response times of each converter. Additionally, EV battery charge acceptance must be accounted for in the SEMS operation to increase the reliability and accuracy of generated solutions. Furthermore, if there is any uncertainty source (e.g., PV, electricity price, etc.) present, forecasting methods should be employed within the SEMS controller.

4.3 SEMS Implementation Using Current Industry Standards

4.3.1 Current Implementation Status of SEMS in EV Charging Industry

Several companies have deployed DC charging plazas, hubs, or sites across the United States. Most of these charging sites use AC-coupled chargers that are powered directly by the AC grid. Electrify America, for example, has installed over 3,500 DC fast chargers at 800 sites [56]. It is not known whether these sites use any form of site energy management software. However, Electrify America has installed 30 MW of battery energy storage systems at more than 140 DC fast charging sites [57]. Therefore, it can be assumed that some form of site energy management is being used. Electrify America's chargers all use OCPP to communicate with a cloud-based CSMS. Tesla Superchargers are another example of widely deployed DC charging plazas. There are over 50,000 Tesla Superchargers installed at thousands of sites around the world [58]. There is no word on whether the new V4 Supercharger stations will be AC- or DC-coupled. Tesla Supercharger sites with on-site battery ESS use Tesla's energy software platform for the site energy management [59].

One of the commercial solutions that is of interest to this study is Ampcontrol's Charging Management System [60]. Ampcontrol's Charging Management System platform uses artificial intelligence to optimize EV charging and energy management for charging site operators. This solution helps businesses reduce energy costs and avoid delays while ensuring reliable charging operations. By scheduling charging sessions intelligently and avoiding peak demand periods, Ampcontrol minimizes energy consumption and ensures timely vehicle departures.

Another commercial solution is BP Pulse's Omega platform [61]. The Omega platform is marketed toward fleet charging, where the site owner also owns the vehicles. However, the platform could potentially be deployed at a DC-coupled charging hub. The Omega charge management system incorporates an on-site component known as the site controller, which serves as the foundation of a comprehensive fleet management ecosystem. By leveraging the site controller, site owners can collect critical data and telemetry at the edge of their operations and seamlessly communicate it to the cloud-based Omega software. The site controller integrates with charge stations and site auxiliary meters to provide the local controller with the power and energy information needed to perform site energy management. The cloud-based Omega software can interface with the site's local utility and enable grid services (demand response, V2G, pricing, etc.).

It is also important to consider the potential benefits of commercial building energy management systems. These systems can help effectively manage energy consumption on-site. However, with EV charging being a crucial aspect of this study, it is essential that any building energy management system selected fully supports the OCPP. It is not yet clear whether current commercial offerings meet this requirement; further investigation is needed. Commercial building energy management system offerings often have more advanced features and support, as well as the ability to integrate with other building management systems. Some well-known commercial solutions include Desigo CC from Siemens [62], EcoStruxure Platform from Schneider Electric [63], Forge Platform from Honeywell [64], and Metasys from Johnson Controls [65].

4.3.2 Approach for an Open-Source SEMS Solution

The alternative to commercial solutions is an open-source approach. Open-source software solutions are gaining popularity due to their flexibility, customization options, and cost-effectiveness. OpenEMS is a widely used open-source platform designed for monitoring and controlling energy systems in buildings and data centers [66]. Given its open-source nature, it has the potential to be utilized within the eCHIP SEMS. OpenFMB is also gaining popularity with utilities to integrate edge devices into a message bus for easy monitoring and control.

There are advantages and disadvantages when taking an open-source approach to site energy management. The advantages are:

- Potential for cost savings due to free or low-cost open-source software
- High customizability and ability to tailor software to specific needs
- Potential for collaboration and innovation with a community of contributors.

On the other hand, the disadvantages are:

- Lack of vendor support and reliance on community forums and documentation for troubleshooting
- Limitations in integration with proprietary software, reducing functionality in certain situations.

4.3.3 An Open-Source SEMS Platform Envisioned for the eCHIP Project

Early web developers popularized the open-source LAMP stack for building/hosting websites. LAMP stands for Linux (operating system), Apache (web server), MySQL (database), and Python/Perl/PHP (programming languages). In the early days of the internet, the LAMP stack played a pivotal role in streamlining a convoluted technology landscape. Much like the LAMP stack, the MING stack is contributing to the simplification of IoT platform deployment. MING stands for MQTT (communication broker), InfluxDB (time-series database), Node-RED (transform data/protocols), and Grafana (visualize data). The acronym was created by Balena in 2019, but the use of these open-source projects to create an IoT system was in use well before then [67].

Recognizing this opportunity in the IoT space, an IoT Common Integration Platform called CIP.io (pronounced "sip-e-o"), was developed in 2016 by ANL [68]. The CIP.io framework has been deployed at the Smart Energy Plaza at ANL, and a containerized version of the CIP.io is available as open-source software [69]. CIP.io incorporates the MING stack, but it also provides example flows. Most importantly, it helps simplify the inclusion of standard communication nodes such as Modbus, OCPP, and OpenADR into the Node-RED flow framework. The framework includes an installation script that provides an easy way to elect which other useful tools will be deployed, such as a docker management tool (Portainer), choice of Influx versions (1.8 or 2.0), and optional inclusion of MongoDB as an additional database tool.

IBM's Node-RED is a vital component in CIP.io. Node-RED is an open-source programming tool with a flow-based approach that enables users to create event-driven applications and automate tasks without writing complex code [70]. Through its web-based interface, users can visually construct flows by dragging and dropping nodes onto a canvas and connecting them. Each node represents a specific function and can be linked to create a sequence of actions triggered by events such as MQTT messages, database changes, and sensor readings. Node-RED is popular in the IoT space for quickly prototyping and deploying IoT applications due to its user-friendly design and extensibility through numerous prebuilt nodes and plugins. We developed and contributed numerous nodes to the Node-Red community [71]. One of the most significant nodes is the node-red-contrib-ocpp node(s), which enables the creation of OCPP-compliant applications [72].

4.3.4 Open-Source SEMS Implementation at eCHIP

The initial plan for the eCHIP SEMS is to take an open-source approach. The high degree of customization for tailoring the software to the needs of this study, in addition to our team's vast experience with open-source IoT projects, led to this decision. CIP.io has very low system requirements and can be fully deployed on a single-board computer system such as a Raspberry Pi or ODroid. For eCHIP, it is highly recommended to use a small-form-factor computer such as the Intel NUC or Dell OptiPlex microcomputer, since they provide more options for performance, scalability, and reliability. The initial architecture of the SEMS will focus on a rule-based control architecture, with plans to explore other architectures later in the project. Future work on this project could also facilitate exploring other commercial or open-source approaches.

It can be noted that all communication to and from the SEMS will be on an IP-based network. This includes TCP/IP, HTTP, WebSockets, and MQTT. Any special hardware needing to communicate with the SEMS that does not support an IP-based network architecture may require intermediary hardware to translate from non-IP-based communication to IP-based communication on the SEMS side. This is possible to implement using the open-source approach, since the architecture of the SEMS is modular and scalable.

The SEMS will ru,n on a Linux-based operating system which will be used as the host operating system to support other containerized applications and services. All containerized applications and services will be freely available open-source programs or custom applications written in-house, except for edge cases where only commercially available applications will suffice to meet the needs of the SEMS.

The SEMS will support multiple databases (InfluxDB, MongoDB, etc.) to store important data that is being monitored in real time, as well as any configuration and access control information. The historical and real-time data can be visualized using the open-source platform Grafana. It provides dashboards that are easily accessible over the web, allowing for a visual demonstration if needed.

5 Component and System Hardware and Software Functionality Testing for the DC Hub

5.1 DC Hub Functionality Testing

The DC hub testbed is developed with an incremental approach, phasing in bus nodes and node types to get closer to a real-world representation of a high-power DC charging hub. The testbed configurations and results are discussed in this section.

5.1.1 Single Charger, Single EV Configuration

The single charger, single EV testbed configuration, shown in Figure 15, comprises the following components, which were described in Section 3: Anderson rectifier, DC REDB, Tritium EV charger, and Hyundai Ioniq 5 EV. The setup has multiple scoped data collection points, identified as MP1–MP4. In addition, data from the site-level controller (CPU1), MQTT Broker (CPU2), OCPP Server (CPU3), and vehicle diagnostics (E3) are all logged and identified as LD1–LD4.

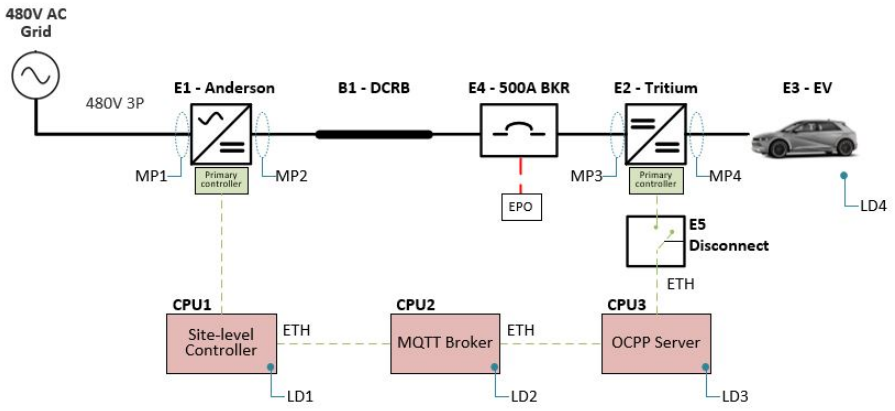

Figure 15. Single charger, single EV configuration

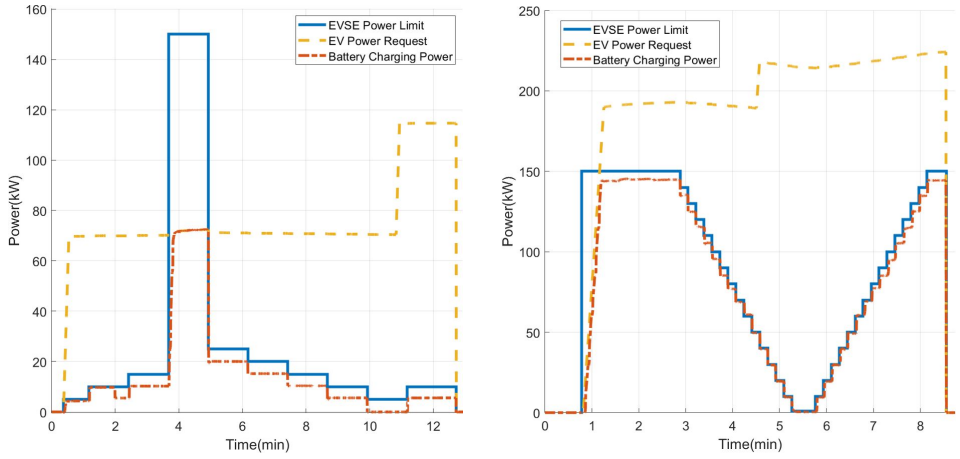

(a) Charging power reference updated every 1 min

(b) Charging power reference updated every 5 s

Figure 16. Single charger, single EV configuration: dynamic charging test results

The considered SEMS behaviors for this use case emulate updating of the power reference for the charger dynamically during a charging session. This scenario emulates a real-time set-point updating of an optimization algorithm. For this scenario, the EVSE power limit is first updated once per minute during the charge session. The EVSE is

expected to constrict the EV to the reference power and update the power value seamlessly. The results of this use case are presented in Figure 16a. The EV's charging power consistently remains below the dynamic power reference communicated by the SEMS to the charger. Then, the same procedure is also followed for every ten seconds and is shown in Figure 16b.

This test case validates capability of the power-hardware-in-the-loop (P-HIL) setup to accommodate fast SEMS transitions. One observation of the test has been that the ramp-up rate is limited more than ramp-down.

5.1.2 Single Charger, Dual EV Configuration

The COTS EVSE has the feature of charging two cars concurrently, one through the CCS1 connector and the other through CHAdeMO. For the setup, both the Hyundai Ioniq 5 (CCS1) and Nissan Leaf (CHAdeMO) are used. The emulated SEMS is expected to control the power limits of the two ports. This experiment also emphasizes the ability to connect and control more than one EV with a single EVSE on the DC hub. The testbed configuration is shown in Figure 17. Note that Tritium PKM150 has a modular DC-DC converter structure that allows charging of both vehicles with different pack voltages at the same time. This is achieved by using different DC-DC converters for the two EVs.

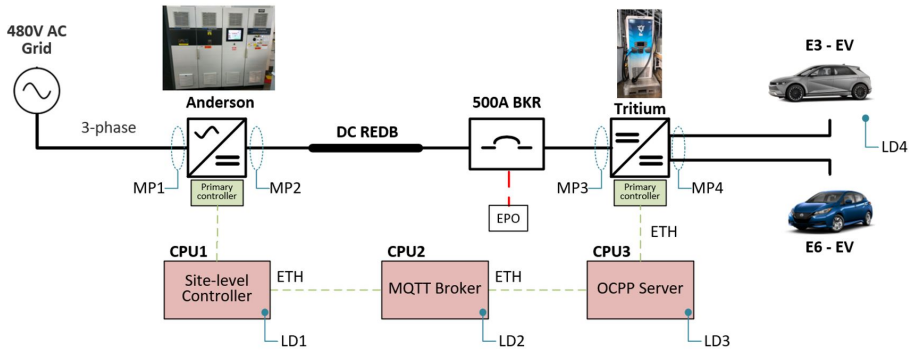

Figure 17. Single charger, dual EV configuration

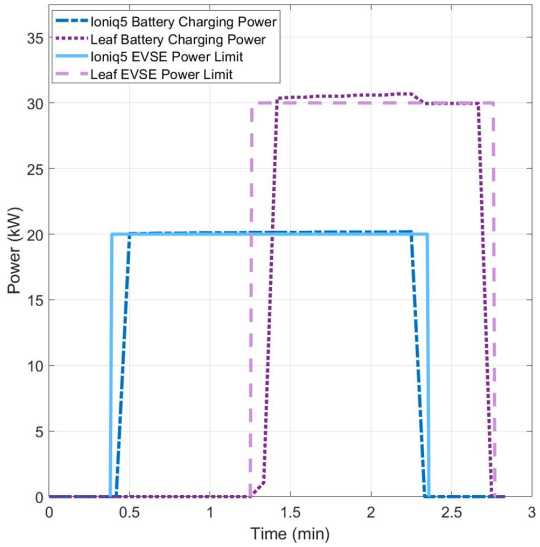

Figure 18. Single charger, dual EV configuration: static charging test results

The results of the static charging test can be observed in Figure 18. The power-limiting command restricts the Ioniq 5 charging at 20 kW and Leaf at 30 kW, concurrently. Though the charging capability of both EVs is higher due to the applied power control of the emulated SEMS through OCPP, both power profiles are restricted to the reference

power commands. This provides the P-HIL setup with the characteristics of port-level power control implementation for future expanded experimental setup.

5.1.3 DC Hub with EV and Battery ESS Emulation

The developed DC charging setup for this use case is shown in Figure 19. For this test, the Anderson AC2660P inverter/rectifier, DC REDB, Tritium PKM150, Hyundai Ioniq 5, and a battery ESS emulator (OPAL RT 5700 and NHR 9300) are used. The specifications of the equipment were introduced in Section 3. This use case demonstrates the grid integration capability of the DC hub platform with the help of the battery ESS. During a demand response event, the SEMS controller adjusts the inverter power output to meet the specified load reduction. The rest of the DC hub will adjust according to the developed rule-based SEMS controller, which will be explained later.

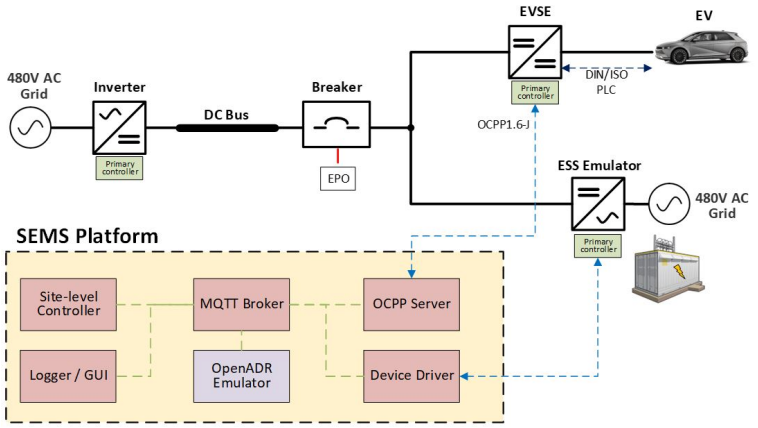

Figure 19. DC charging hub configuration and SEMS platform implementation with EV and battery ESS

This use case presents the following implementation example. Utilities commonly use the openADR protocol (explained in Section 2.5.6) to implement automated demand response. Automated demand response may be realized as part of a broader advanced distribution management system (ADMS) or DERMS. The test case emulates an openADR "fast demand response" event using an openADR 2.0b profile. A "LOAD_DISPATCH" signal of signal type "multiplier" is used to specify a 50% load reduction. Many other signal types and use cases are possible under the openADR protocol, e.g. other means of load control, energy storage charge/discharge control, and communication of electricity pricing.

The following rule-based controller is implemented. The SEMS will charge the EVs as soon as possible, with the inverter supplying power to the EV first. If the inverter supply is not enough, the ESS will provide the remaining power. If both the inverter and the ESS are not sufficient to meet load, then EV charging power will be reduced. If there is generation on the DC hub, it will be offered to the ESS first, and then the inverter will feed it back to the grid if necessary.

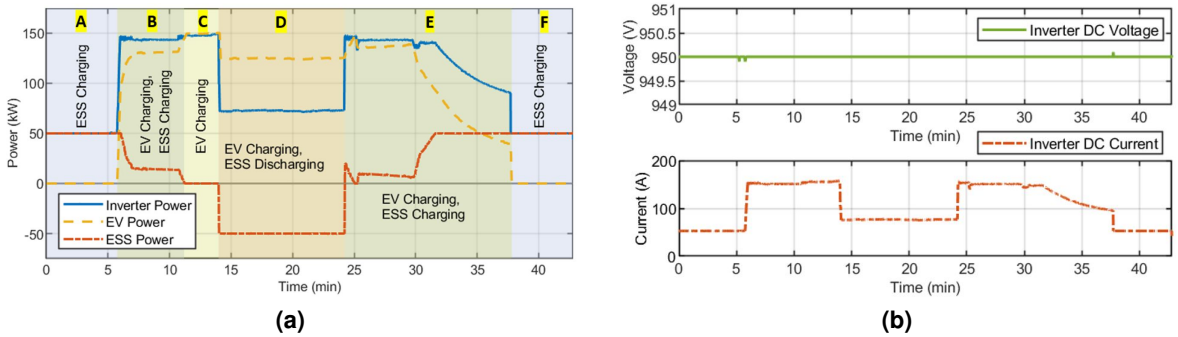

Figure 20. DC hub operation w/ EV and ESS under a rule-based SEMS

Figure 20 shows the experimental results of the operation. In region A, there is no EV connected to the charger. The ESS is charged from the grid connection via the central inverter. An EV connects and charges in regions B through E. In region B, the EV charging power is slightly less than the inverter capacity, and the ESS continues charging with the remaining available inverter power. In region C, the EV charges around 150 kW, so the ESS is idle. The demand response event occurs in region D. The available inverter capacity is reduced by the SEMS by 50% from 150 kW to 75 kW. The ESS discharges at rated capacity to support EV charging at around 125 kW. In region E, the inverter capacity returns to 150 kW, following the demand response event. The EV can again charge up to 150 kW. As EV reaches top of charge curve, charging power reduces, and the ESS again charges with the remaining available inverter power. In region F, the EV is disconnected, having reached an 80% state of charge. The ESS continues recharging from the inverter at 50 kW. The corresponding inverter DC voltage and DC current output are also shown in the same figure. The inverter output voltage is tightly regulated at 950 VDC.

5.1.4 DC Hub with EV, Battery ESS, and PV Emulation

This use case demonstrates the DC hub with EV, ESS, and PV generation. The types of the equipment are the same with the previous use case. PV generation is implemented with the hardware, as explained in Section 3. For the PV generation, a 1-second resolution PV power generation is used to capture the fast-timescale effects of PV generation variability [54]. Again, a rule-based SEMS is used to control the DC hub power flow appropriately. The SEMS dispatches ESS power in response to measured EV charging power and measured PV generation. Figure 21 shows the configuration of the hardware setup.

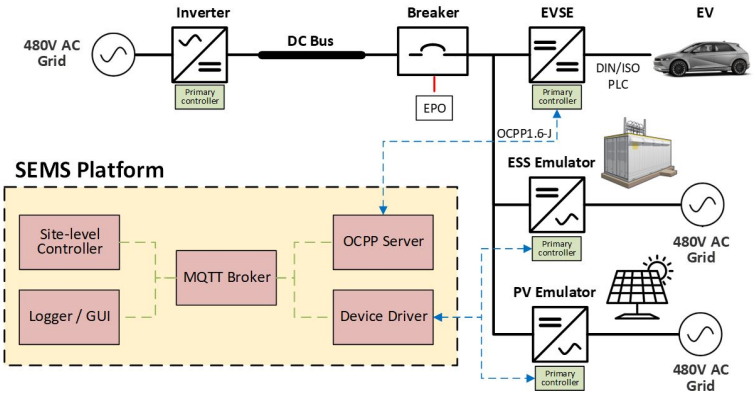

Figure 21. DC charging hub configuration and SEMS platform implementation with EV, battery ESS, and PV

The following rule-based controller is implemented: ESS power is dispatched according to the difference between measured PV generation and measured EV charging power. Energy storage tries to capture any PV generation in excess of the charging load. When plugged in, EV charging power is first supplied by the PV generation, then the ESS, then the inverter only if the PV generation and ESS capacity are insufficient. This realizes maximum internal consumption of the PV generation while reducing the peak power demand from the utility, leading to higher efficiency operation and reduced electricity costs (reduced energy and power demand). If there is net generation on hub, it will be offered to the ESS first, and then the inverter will supply it back to the grid if necessary.

Figure 22 shows the results of the test. In regions A and B, there is no EV connected to the charger. In region A, all of the PV generation is used to charge the ESS. In region B, the ESS has reached its max state of charge, and the PV generation is fed back to the grid. Then, the EV connects and charges through region C. In this region, all the PV generation is used to directly charge the vehicle. Any outstanding charging demand is then supplied first by the ESS, then from the grid via the central inverter as required. In region D, the EV has completed charging. The PV generation is used to recharge the ESS, similar to region A.

PV generation can recharge the ESS during light loading periods, while directly supplying power to EV chargers during high demand periods. This internal transfer of generated energy is more efficient in the DC hub solution due to reduced conversion stages. Peak power demand from the grid is significantly reduced. If the ESS is full, feeding generated power back to the grid is accomplished.

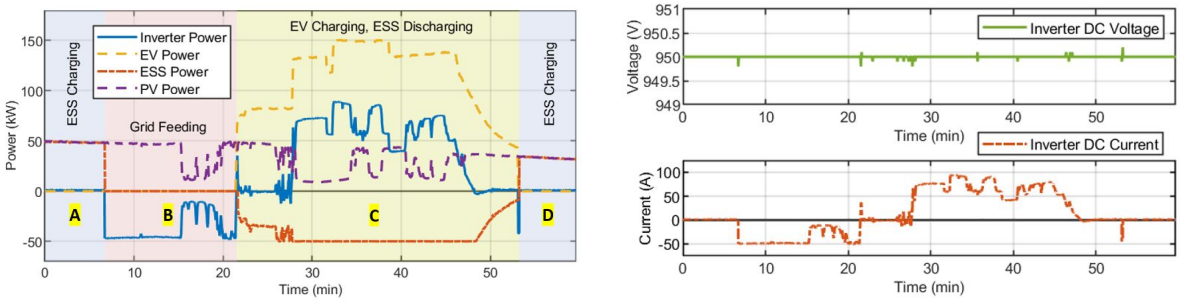

Figure 22. DC hub operation w/ EV, ESS, and PV under a rule-based SEMS

5.1.5 DC Hub with EV, Battery ESS, PV, and Building Load Emulation

This use case demonstrates a DC hub with EV fast charging, ESS, PV generation, and building load. The types of the equipment are the same as with the previous use case. Building load emulation is implemented with the hardware as explained in Section 3. Building load data with 1-second resolution is used for this use case [55]. A rule-based SEMS is used to control the DC hub power in an appropriate manner. The SEMS dispatches ESS power in response to measured PV generation and DC hub loads. Figure 23 shows the configuration of the hardware setup.

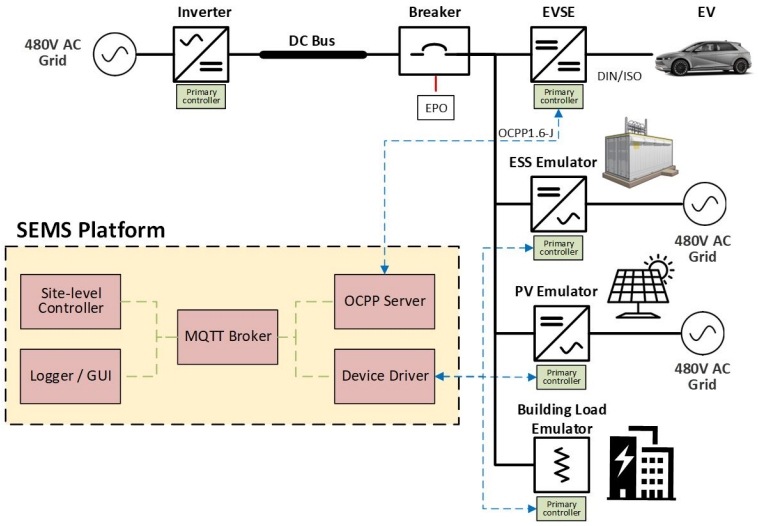

Figure 23. DC charging hub configuration and SEMS platform implementation with EV, battery ESS, PV, and building load

The following rule-based controller is implemented: ESS power is dispatched according to the difference between measured PV generation and measured combined load power. Energy storage tries to capture any PV generation in excess of the total DC hub loads. EV charging power and building loads are first supplied by the PV generation, then the ESS, then the inverter only if the PV generation and ESS capacity are insufficient. This realizes maximum internal consumption of the PV generation while reducing the peak power demand from the utility, leading to higher efficiency operation and reduced electricity costs (reduced energy and power demand). If there is net generation on hub, it will be offered to ESS first, and then inverter will supply it back to the grid if necessary.

Figure 24 shows the results of the test. In regions A through C, there is no EV connected to the charger. In region A, PV generation supplies the building load and recharges the ESS. In region B, the ESS has reached its max state of charge, and the excess PV generation is fed back into the grid. In region C, the PV generation intermittently drops below the building load power, leading to the ESS discharging and charging in response. An EV connects and

charges through region D. PV generation is fully utilized within the DC hub for supplying the building load or EV charger. Remaining load demand is first supplied by the ESS, then from the grid via the central inverter as required. In region E, the EV has completed charging. The PV generation supplies the building load and recharges the ESS with any remaining generation.

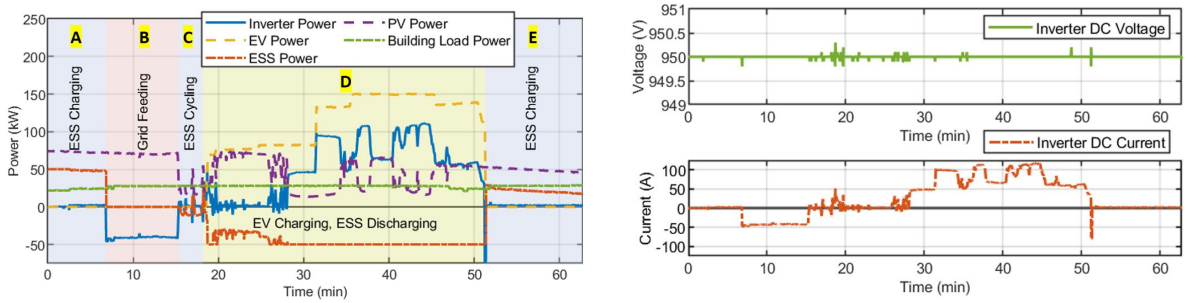

Figure 24. DC hub operation w/ EV, ESS, PV, and building load under a rule-based SEMS

5.2 ORNL UPER DC-DC Charger Testing Results

The fully assembled 175 kW, 1000 V class charger was previously described in Section 3.2 and shown in Figure 5. In this section, the charger is powered and tested at 950 V and 150 A, which approximately corresponds to 150 kW of steady-state operation. The important waveforms corresponding to the UPER operation are shown in Figure 25.

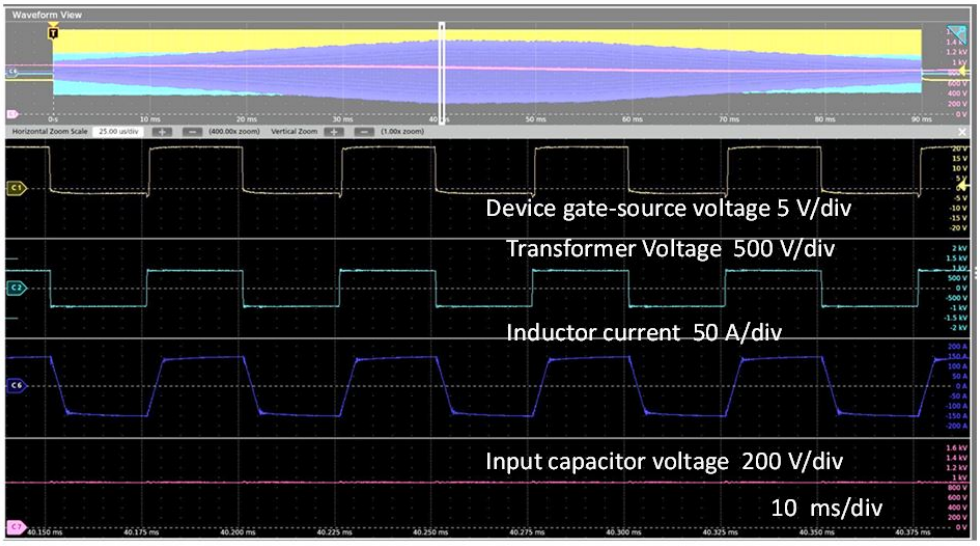

Figure 25. UPER charger test results at 950 V and 150 A

The lower current testing results to demonstrate ZVS operation are shown in Figure 26.

The ANL-developed SpEC module was selected to act as an interface between the ORNL UPER and the external components, which are the EV and the SEMS platform. The interface between UPER and SPEC is implemented over a CAN, and the protocol is developed in a collaborative way. To test the developed SpEC-UPER interface, the UPER was deployed in the setup developed at ORNL shown in Figure 27.

The two sources act as DC bus and vehicle emulator. The SpEC is represented by an equivalent database CAN (DBC) file while the actual testing and integration of UPER-SpEC integration will be done in the future. The test

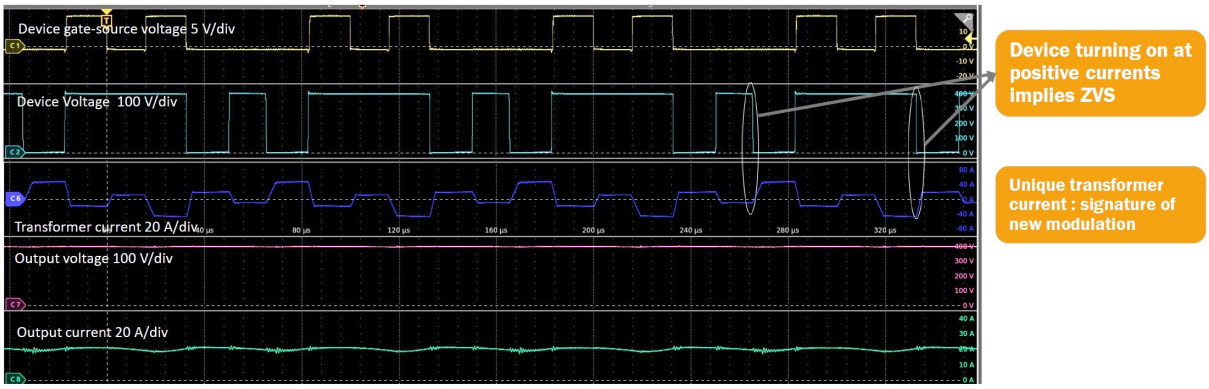

Figure 26. UPER charger testing results at 400 V and 20 A: ZVS operation at low currents

results attained are shown in Figure 28. In this test, the commands are sent by the SPEC equivalent DBC file. All the relevant modes such as cable check, precharge, voltage, and current regulation, and shutdown are tested successfully.

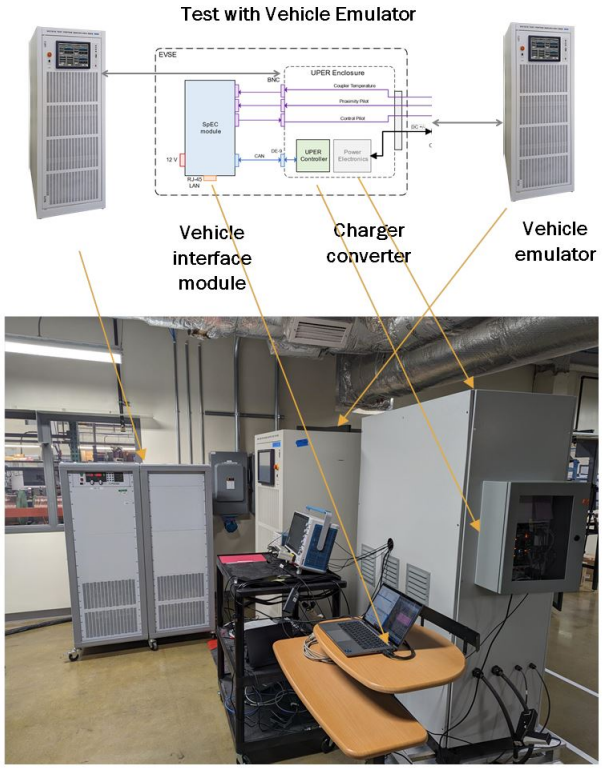

Figure 27. UPER-SpEC integration setup

5.3 Bidirectional Power Transfer Demonstration at ANL

In the pursuit of developing and showcasing DC V2G capabilities at the component level, several achievements were attained. We completed a major milestone by creating an ISO 15118-2 bidirectional power transfer (BPT) stack for the SpEC II communication controller, a crucial step towards enabling V2G capabilities on SpEC-based DC chargers. Simultaneously, we designed a custom MQTT protocol for the SpEC-based DC charger, allowing previously unavailable information exchange beyond the OCPP 1.6J standard. This protocol opens doors for advanced SEMS strategies within the eCHIP framework. Furthermore, the protocol was used to develop a real-time visualization dashboard for monitoring and controlling SpEC-based DC chargers.

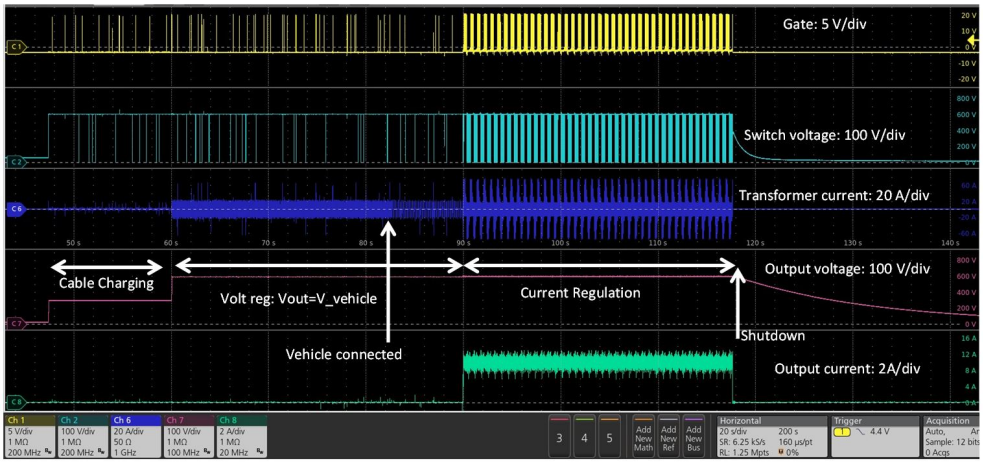

Figure 28. UPER-SpEC interface testing results at 600 V and 10 A

ANL also formed a partnership with Lion Electric, culminating in a compelling demonstration at the Fall 2023 EVs@Scale Semi-Annual meeting hosted at ANL [73]. Leveraging the AeroVironment ABC-170 as the power source and pairing it with the SpEC II module, we successfully conducted a V2G session with the Lion Bus, demonstrating rapid switching between charging and discharging in real time using the dashboard. This demonstration underscores the practical application and promise of these cutting-edge developments in EV charging and vehicle grid integration. The setup for the demonstration is shown in Figure 29.

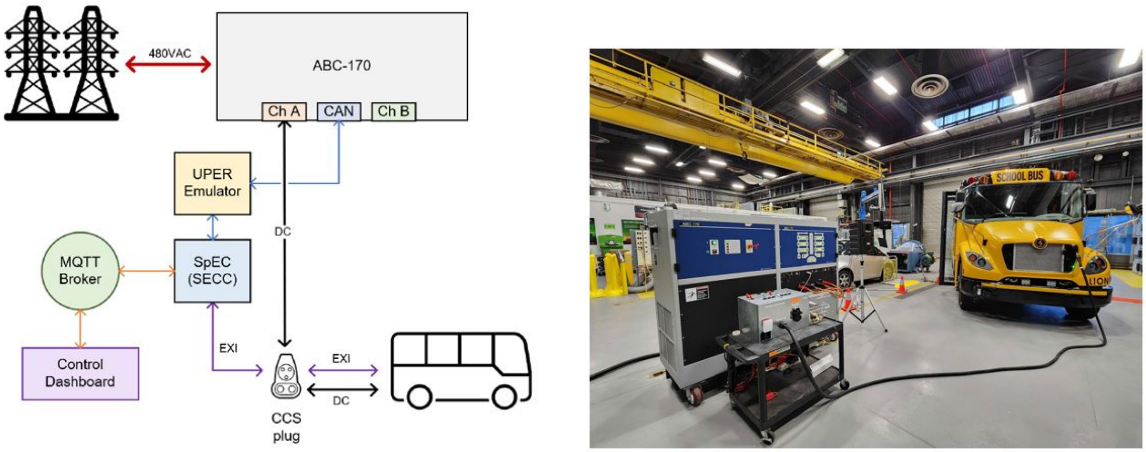

(a) **(b)**

Figure 29. Demonstrating a V2G session with the Lion Electric Bus at ANL: a) system configuration, b) experimental setup

6 Conclusion and Future Work

This report summarized the development process of a DC charging hub approach mostly using COTS solutions. The developed platform is instrumental in facilitating rigorous testing of various COTS devices, as well as enabling the implementation and assessment of SEMS controllers at the rated power scale. This study will set the stage for smooth incorporation into real-world EV charging scenarios operating under the DC hub approach.

First, we surveyed the available industry solutions and standards that are similar to the problem we are addressing under the eCHIP project and listed our findings. Then, the report provided eCHIP team's approach to building the DC charging hub experimental platform, both from hardware and software points of view. We explained available COTS hardware and software solutions that we used for the purpose of building the DC hub. Detailed discussions are also provided for in-house developed power and control hardware components. Finally, the discussion of how to control the charging facility and how to implement site energy management using open source solutions have been covered. Preliminary hardware testing results are also included.

Future work will include demonstration of more advanced SEMS controllers that will focus on optimized and distributed operation of the site components. Furthermore, the bottom-up integration approach of an in-house developed ORNL DC-DC UPER charger with ANL's SpEC Module into the developed DC charging hub at NREL will be discussed in a future study. The charging hub will integrate with more nodes that include COTS DC-DC chargers to cover more use cases, including V2X operation within the hub with applicable EVs.

References

1 *Electric Vehicles at Scale Consortium*. 2023. URL: https://www.energy.gov/eere/vehicles/electric-vehicles-scale-consortium. [Online; accessed 14-Apr-2023].

2 *Electrification 2022 Annual Progress Report*. 2023. US DOE Vehicle Technologies Office. URL: https://www.energy.gov/sites/default/files/2023-10/VTO_2022_APR_ELECTRIFICATION_DRAFT%20REPORT_compliant_-min.pdf. [Online; accessed 16-Dec-2023].

3 Rivera, Sebastian et al. June 2021b. "Electric vehicle charging infrastructure: From grid to battery." *IEEE Ind. Electron. Mag.* 15 (2): 37–51.

4 Franzese, Pasquale et al. Sept. 2023. "Fast DC charging infrastructures for electric vehicles: Overview of technologies, standards, and challenges." *IEEE Trans. Transp. Electrific.* 9 (3): 3780–3800.

5 Sannino, A., Postiglione, G., and Bollen, M.H.J. Sept. 2003. "Feasibility of a DC network for commercial facilities." *IEEE Trans. Ind. Appl.* 39 (5): 1499–1507.

6 Bai, Sanzhong, Yu, Du, and Lukic, Srdjan. Sept. 2010. "Optimum design of an EV/PHEV charging station with DC bus and storage system." In: *IEEE Energy Conversion Congr. Expo. (ECCE)*, 1178–1184.

7 Bai, Sanzhong and Lukic, Srdjan. Sept. 2011. "Design considerations for DC charging station for plug-in vehicles." In: *IEEE Vehicle Power Propulsion Conf. (VPPC)*, 1–6.

8 Deb, Naireeta et al. 2021. "A review of extremely fast charging stations for electric vehicles." *Energies* 14 (22): 7566.

9 Bai, Sanzhong and Lukic, Srdjan M. 2013. "Unified active filter and energy storage system for an MW electric vehicle charging station." *IEEE Trans. Power Electron.* 28 (12): 5793–5803.

10 Ahmad, Adnan et al. 2022. "An overview on medium voltage grid integration of ultra-fast charging stations: Current status and future trends." *IEEE Open J. Ind. Electron. Soc.* 3: 420–447.

11 Rivera, Sebastian, Wu, Bin, and Kouro, Samir. June 2014. "Distributed dc bus EV charging station using a single dc-link h-bridge multilevel converter." In: *IEEE Int. Symp. Ind. Electron. (ISIE)*, 1496–1501.

12 Hariri, Raghda et al. Oct. 2021. "A survey on charging station architectures for electric transportation." In: *Annu. Conf. IEEE Ind. Electron. Soc. (IECON)*, 1–8.

13 Yong, Jia Ying et al. 2015. "Bi-directional electric vehicle fast charging station with novel reactive power compensation for voltage regulation." *Int. J. Elect. Power & Energy Syst.* 64: 300–310.

14 Ito, Y., Zhongqing, Y., and Akagi, H. Aug. 2004. "DC microgrid based distribution power generation system." In: *Int. Power Electron. Motion Control Conf. (IPEMC)*.

15 Justo, J. J. et al. 2013. "AC-microgrids versus DC-microgrids with distributed energy resources: A review." *Renew. Sustain. Energy Rev.* 24: 387–405.

16 Moorthy, R. S. K. et al. Oct. 2022. "Megawatt scale charging system architecture." In: *IEEE Energy Conversion Congr. Expo. (ECCE)*.

17 Sun, Feng et al. Sept. 2020. "The power electronic transformer based multi-port DC charging station." In: *IEEE Asia-Pacific Power Energy Eng. Conf. (APPEEC)*.

18 Iyer, Vishnu Mahadeva et al. 2020. "An approach towards extreme fast charging station power delivery for electric vehicles with partial power processing." *IEEE Trans. Ind. Electron.* 67 (10): 8076–8087.

19 She, Xu, Huang, Alex Q., and Burgos, Rolando. 2013. "Review of solid-state transformer technologies and their application in power distribution systems." *IEEE J. Emerg. Sel. Topics Power Electron.* 1 (3): 186–198.

20 He, Tingting et al. Oct. 2017. "Comparison study of electric vehicles charging stations with AC and DC buses for bidirectional power flow in smart car parks." In: *Annu. Conf. IEEE Ind. Electron. Soc. (IECON)*.

21 Rivera, Sebastian et al. 2015. "Electric vehicle charging station using a neutral point clamped converter with bipolar DC bus." *IEEE Trans. Ind. Electron.* 62 (4): 1999–2009.

22 Tan, Longcheng et al. 2016. "Effective voltage balance control for bipolar-DC-bus-fed EV charging station with three-level DC–DC fast charger." *IEEE Trans. Ind. Electron.* 63 (7): 4031–4041.

23 Rivera, Sebastian et al. 2021a. "Bipolar DC power conversion: State-of-the-art and emerging technologies." *IEEE J. Emerg. Sel. Topics Power Electron.* 9 (2): 1192–1204.

24 Salomonsson, Daniel, Soder, Lennart, and Sannino, Ambra. 2009. "Protection of low-voltage DC microgrids." *IEEE Trans. Power Del.* 24 (3): 1045–1053.

25 Ali, Zulfiqar et al. 2021. "Fault management in DC microgrids: A review of challenges, countermeasures, and future research trends." *IEEE Access* 9: 128032–128054.

26 Jayamaha, D.K.J.S., Lidula, N.W.A., and Rajapakse, A.D. 2020. “Protection and grounding methods in DC microgrids: Comprehensive review and analysis.” *Renew. Sustain. Energy Rev.* 120: 109631.
27 Paul, D. 2002. “DC traction power system grounding.” *IEEE Trans. Ind. Appl.* 38 (3): 818–824.
28 Mohammadi, Jafar, Badrkhani Ajaei, Firouz, and Stevens, Gary. 2019. “Grounding the DC microgrid.” *IEEE Trans. Ind. Appl.* 55 (5): 4490–4499.
29 Pons, Enrico, Tommasini, Riccardo, and Colella, Pietro. 2017. “Fault current detection and dangerous voltages in DC urban rail traction systems.” *IEEE Trans. Ind. Appl.* 53 (4): 4109–4115.
30 Mobarrez, Maziar et al. 2017. “Grounding architectures for enabling ground fault ride-through capability in DC microgrids.” In: *IEEE Int. Conf. DC Microgrids (ICDCM)*, 81–87.
31 Dragičević, Tomislav et al. 2016. “DC microgrids—part II: A review of power architectures, applications, and standardization issues.” *IEEE Trans. Power Electron.* 31 (5): 3528–3549.
32 *Emerge Alliance Open Industry Association*. 2023. URL: https://www.emergealliance.org/. [Online; accessed 19-Dec-2023].
33 *Current/OS Based DC Microgrids*. 2023. URL: https://currentos.foundation/. [Online; accessed 19-Dec-2023].
34 “Power supply interface at the input to telecommunications and datacom equipment; Part 3: Operated by rectified current source, alternating current source or direct current source up to 400 V; Sub-part 1: Direct current source up to 400 V”. 2021. *ETSI EN 300 132-3-1*.
35 “LVDC distribution systems up to 1500V DC”. 2009. *IEC SMB SG4 working group*.
36 “Medium voltage electric power, direct current”. 2019. *MIL-STD-1399 Section 300, Part 3*.
37 “Preliminary electrical systems design criteria and practices (surface ships) for medium voltage direct current (MVDC) applications”. 2020. *NAVSEA T9300-AF-PRO-510*.
38 “IEEE recommended practice for 1 kV to 35 kV medium-voltage DC power systems on ships”. 2018. *IEEE 1709*.
39 “Railway applications - Supply voltages of traction systems”. 2005. *EVS-EN 50163:2005*.
40 “Railway applications - Supply voltages of traction systems”. 2014. *IEC 60850:2014*.
41 “Railway applications — Fixed installations and rolling stock — Criteria to achieve technical compatibility between pantographs and overhead contact line”. 2022. *BS EN 50367:2020+A1:2022*.
42 “Railway applications-Fixed installations—Part 1: Protective provisions relating to electrical safety and earthing”. 2013. *IEC 62128-1*.
43 “IEEE standard for interconnection and interoperability of distributed energy resources with associated electric power systems interfaces”. 2018. *IEEE 1547*.
44 “Open charge alliance-Open charge point protocol”. 2018. *OCPP 2.0.1*.
45 “Road vehicles vehicle to grid communication interface”. 2022. *ISO 15118-20:2022*.
46 “MODBUS Application Protocol Specification V1.1b3”. 2012. *MODBUS protocol*.
47 “Building automation and control systems (BACS) Part 5: Data communication protocol”. 2022. *ISO 16484-5:2022*.
48 “MQTT Version 5.0”. 2019. *OASIS Standard*.
49 “Open Field Message Bus (OpenFMB) framework”. 2016. *NAESB Standard*.
50 “Common information model schema version 2.54”. 2020. *DMTF CIM Standard*.
51 “Communication networks and systems for power utility automation”. 2023. *IEC 61850:2023*.
52 “IEEE standard for electric power systems communications-distributed network protocol (DNP3)”. 2012. *IEEE 1815-2012*.
53 “Systems interface between customer energy management system and the power management system - Part 10-1: Open automated demand response”. 2018. *IEC 62746-10-1:2018*.
54 Boyd, M., Chen, T., and Dougherty, B. 2017. *NIST campus photovoltaic (PV) arrays and weather station data sets.* [Data set]. https://doi.org/10.18434/M3S67G. National Institute of Standards and Technology. U.S. Department of Commerce, Washington, D.C.
55 Kriechbaumer, T. and Jacobsen, H.A. 2018. *BLOND: Building-level office environment dataset.* [Data set]. https://doi.org/10.14459/2017mp1375836. Technical University of Munich, Munich, Germany.
56 *Electrify America-Fast Facts*. 2024. URL: https://media.electrifyamerica.com/en-us/press-kits/fast-facts. [Online; accessed 15-Jan-2024].
57 *Electrify America Reaches 30 Megawatts in Installed Battery Energy Storage at 140 DC Fast Charging Stations Across the US and Initiates Virtual Power Plant (VPP) Services*. 2021. URL: https://media.electrifyamerica.com/en-us/releases/164. [Online; accessed 15-Jan-2024].

58 *Tesla Supercharger*. 2024. URL: https://www.tesla.com/supercharger. [Online; accessed 15-Jan-2024].
59 *Tesla Energy Software*. 2024. URL: https://www.tesla.com/support/energy/tesla-software. [Online; accessed 15-Jan-2024].
60 *The Software for Electric Vehicle Charging Optimization*. 2024. URL: https://www.ampcontrol.io/smart-charging-software. [Online; accessed 15-Jan-2024].
61 *Charge management software: Put your EV fleet charging on autopilot*. 2024. URL: https://bppulsefleet.com/fleet/products/charge-management-software/. [Online; accessed 15-Jan-2024].
62 *State-of the-art building management system Desigo CC - Integrated Building Management Platform*. 2024. URL: https://www.siemens.com/global/en/products/buildings/automation/desigo/building-management/desigo-cc.html. [Online; accessed 15-Jan-2024].
63 *EcoStruxure Platform*. 2024. URL: https://www.se.com/ww/en/work/campaign/innovation/platform.jsp. [Online; accessed 15-Jan-2024].
64 *Honeywell Forge*. 2023. URL: https://www.honeywellforge.ai/. [Online; accessed 20-Jan-2024].
65 *METASYS Building Automation System*. 2024. URL: https://www.johnsoncontrols.com/building-automation-and-controls/building-management/building-automation-systems-bas. [Online; accessed 15-Jan-2024].
66 *Github-OpenEMS*. 2024. URL: https://github.com/OpenEMS/openems. [Online; accessed 15-Jan-2024].
67 *Github-MING*. 2024. URL: https://github.com/DynamicDevices/ming. [Online; accessed 15-Jan-2024].
68 *Vehicle Systems 2016 Annual Report*. 2016. US DOE Vehicle Technologies Office. URL: https://www.energy.gov/eere/vehicles/articles/vehicle-systems-2016-annual-progress-report. [Online; accessed 15-Jan-2024].
69 *GitHub-Argonne National Laboratory/CIP.io*. 2024. URL: https://github.com/Argonne-National-Laboratory/CIP.io. [Online; accessed 15-Jan-2024].
70 *Node-RED: Low-code programming for event-driven applications*. 2024. URL: https://nodered.org/. [Online; accessed 15-Jan-2024].
71 *jayharper*. 2024. URL: https://www.npmjs.com/~jayharper. [Online; accessed 15-Jan-2024].
72 *node-red-contrib-ocpp (node) - Node-RED*. 2024. URL: https://flows.nodered.org/node/node-red-contrib-ocpp. [Online; accessed 15-Jan-2024].
73 *EVs@Scale Lab Consortium Semi-Annual Stakeholder Meeting*. 2023. URL: https://www.anl.gov/taps/evsatscale. [Online; accessed 14-Apr-2023].

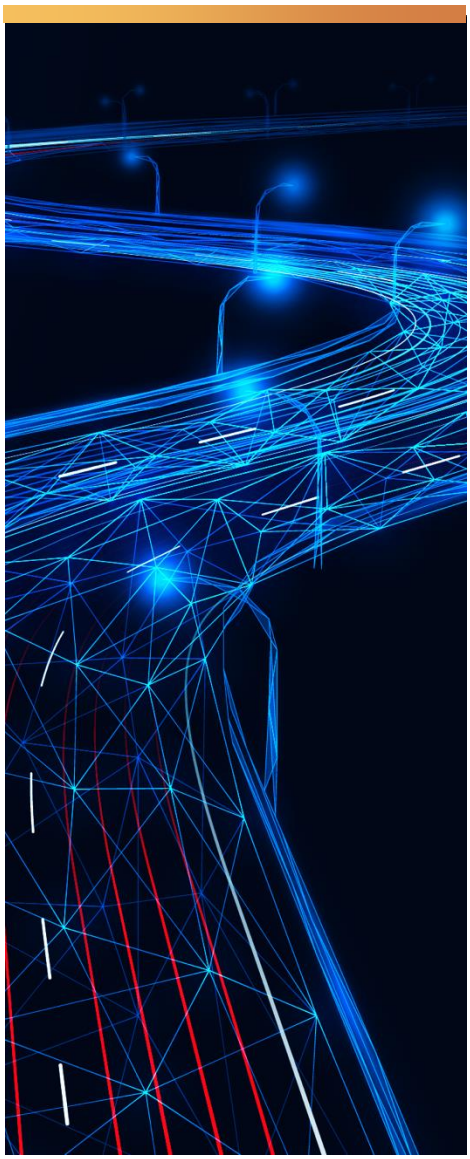

EVs@Scale

U.S. Department of Energy

U.S. DEPARTMENT OF ENERGY | *Office of* ENERGY EFFICIENCY & RENEWABLE ENERGY

For more information, visit:
energy.gov/eere/vehicles/electric-vehicles-scale-consortium

DOE/GO-102024-5919 • April 2024